哈密顿有效场论研究格点能谱

吴佳俊 (国科大)

Collaborator: T.-S. H. Lee, D. B. Leinweber, Z.-W. Liu (刘占伟), M. Oka, A. W. Thomas, G.-J. Wang(王广娟), R. D. Young, Y. Li(李严), Z. Yang(杨智), S.-I. Zhu(朱世琳)

理论所 强子质量的非微扰起源 2023. 4. 25

Outline

- Motivation
- Hamiltonian Effective Field Theory (HEFT)
- Study N*(1535), N*(1440), Λ*(1405)
- Study $D_{s0}(2317)$, $D_{s1}(2460)$, $D_{s1}(2536)$, $D_{s2}(2573)$
- Predict $B_{s0}(5730)$, $B_{s1}(5770)$
- Summary

Motivation

Partial Wave Analysis
With various Model:
Such as Breit-Wigner Form, Flatte Form, Coupled Channel Form, and so on

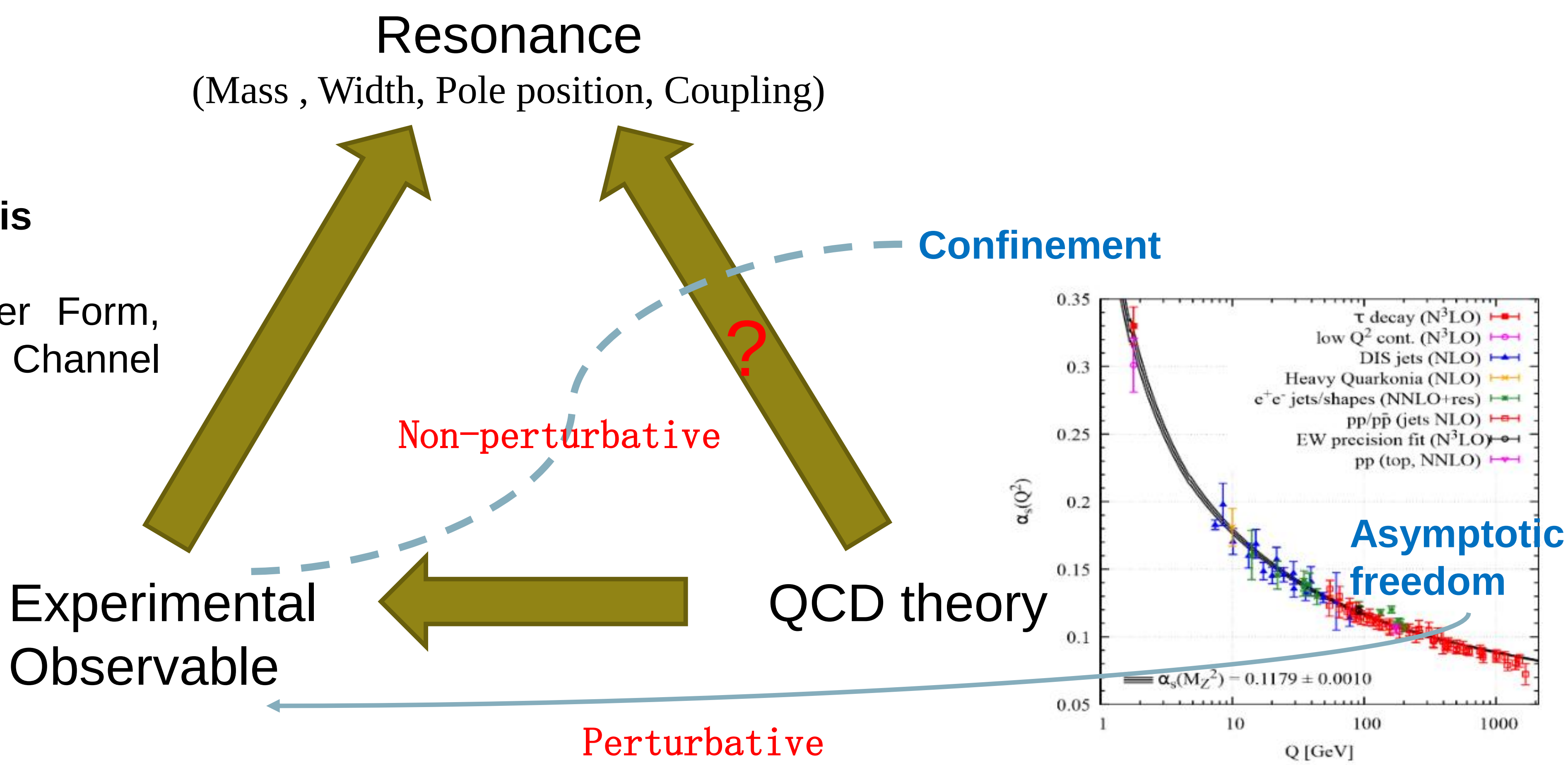

Resonance

(Mass , Width, Pole position, Coupling)

Experimental Observable

(Differential Cross Sections)

QCD theory

Resonance
(Mass , Width, Pole position, Coupling)

T matrix
(Phase Shifts,
inelasticity)

Partial Wave Analysis

Experimental Observable
(Differential Cross Sections)

QCD theory

Resonance

(Mass , Width, Pole position, Coupling)

T matrix
(Phase Shifts, inelasticity)

Partial Wave Analysis

Experimental Observable
(Differential Cross Sections)

Lattice QCD

Non-perturbative

QCD theory

Resonance
(Mass , Width, Pole position, Coupling)

T matrix
(Phase Shifts, inelasticity)

Partial Wave Analysis

Experimental Observable
(Differential Cross Sections)

Lattice QCD

Non-perturbative

QCD theory

Lattice QCD

1. QCD theory: on a box in the Euclid four space

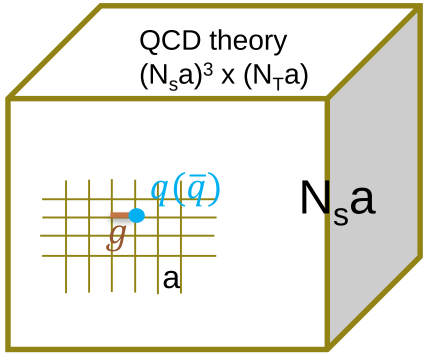

2. a -> UV cutoff, $N_s a$ -> Infrared truncation
3. Lattice QCD -> a model of statistical physics.

$$\langle O \rangle = \int D\phi O[\phi] P[\phi] \qquad P[\phi] = \frac{1}{Z} e^{-S[\phi]} \qquad Z = \int D\phi e^{-S[\phi]}$$

Φ: field quantity, *S*[*ϕ*]: Action, *O*[*ϕ*]:physical quantity

4. Monte Carlo method
5. Three steps for Lattice QCD to real world

a， Configuration

b， Measurement $\sum_{(\vec{y}-\vec{x})\in Z^3} e^{i\vec{p}.(\vec{y}-\vec{x})} \left\langle T\left(\psi(t;\vec{y}),\psi^\dagger(t;\vec{y})\right)\right\rangle \sim \sum_{\Gamma,i} Z_i^\Gamma e^{-E_i^\Gamma t}$

c， Transformation

Resonance

(Mass , Width, Pole position, Coupling)

Lattice QCD

T matrix

(Phase Shifts, inelasticity)

Partial Wave Analysis

Experimental Observable

(Differential Cross Sections)

Lattice Spectrum

Lattice QCD

Non-perturbative

QCD theory

1. QCD theory: on a box in the Euclid four space

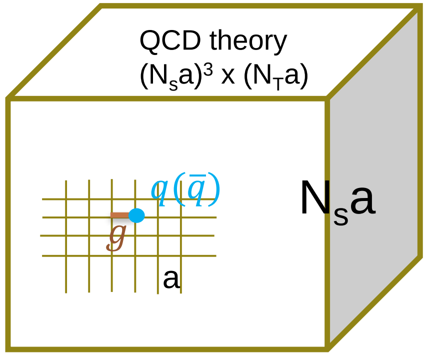

2. a -> UV cutoff, $N_s a$ -> Infrared truncation
3. Lattice QCD -> a model of statistical physics.

$$\langle O \rangle = \int D\phi O[\phi] P[\phi] \qquad P[\phi] = \frac{1}{Z} e^{-S[\phi]} \qquad Z = \int D\phi e^{-S[\phi]}$$

Φ: field quantity, *S*[*ϕ*]: Action, *O*[*ϕ*]:physical quantity

4. Monte Carlo method
5. Three steps for Lattice QCD to real world

a, Configuration

b, Measurement $\sum_{(\vec{y}-\vec{x})\in Z^3} e^{i\vec{p}\cdot(\vec{y}-\vec{x})} \langle T(\psi(t;\vec{y}),\psi^\dagger(t;\vec{y}))\rangle \sim \sum_{\Gamma,i} Z_i^\Gamma e^{-E_i^\Gamma t}$

c, Transformation

Resonance

(Mass , Width, Pole position, Coupling)

T matrix
(Phase Shifts, inelasticity)

Lüscher's Method

M. Luscher, NPB 354, 531 (1991).

Partial Wave Analysis

Experimental Observable
(Differential Cross Sections)

Lattice Spectrum

Lattice QCD

Non-perturbative

QCD theory

Lattice QCD

1. QCD theory: on a box in the Euclid four space

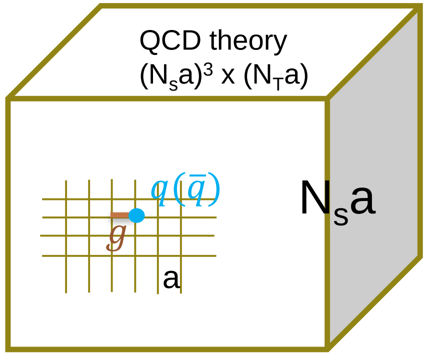

2. a -> UV cutoff, $N_s a$ -> Infrared truncation
3. Lattice QCD -> a model of statistical physics.

$$\langle O \rangle = \int D\phi O[\phi] P[\phi] \qquad P[\phi] = \frac{1}{Z} e^{-S[\phi]} \qquad Z = \int D\phi e^{-S[\phi]}$$

Φ: field quantity, $S[\phi]$: Action, $O[\phi]$:physical quantity

4. Monte Carlo method
5. Three steps for Lattice QCD to real world

a, Configuration

b, Measurement $\sum_{(\vec{y}-\vec{x})\in Z^3} e^{i\vec{p}.(\vec{y}-\vec{x})} \langle T(\psi(t;\vec{y}),\psi^\dagger(t;\vec{y}))\rangle \sim \sum_{\Gamma,i} Z_i^\Gamma e^{-E_i^\Gamma t}$

c, Transformation

How to use **Lüscher's Method** ？

ππ –> ππ & ππ –> $\bar{K}K$ & $\bar{K}K$–> $\bar{K}K$

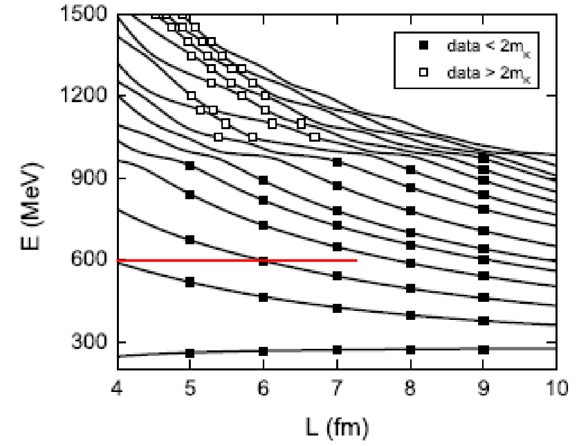

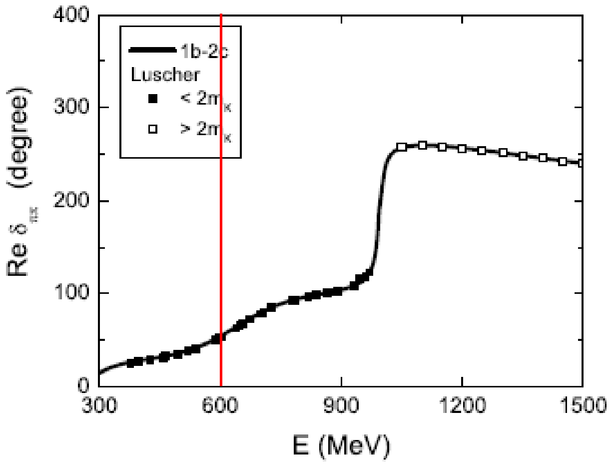

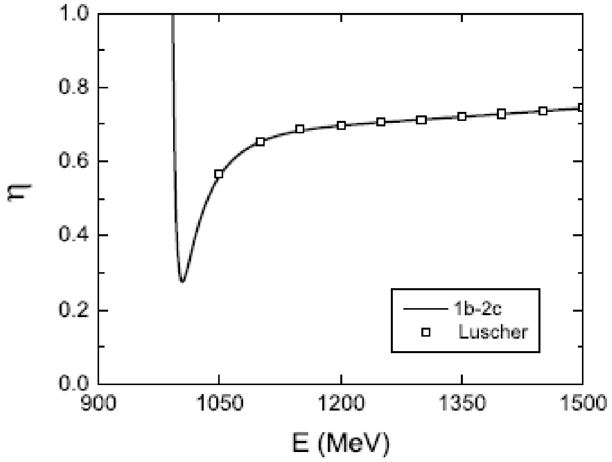

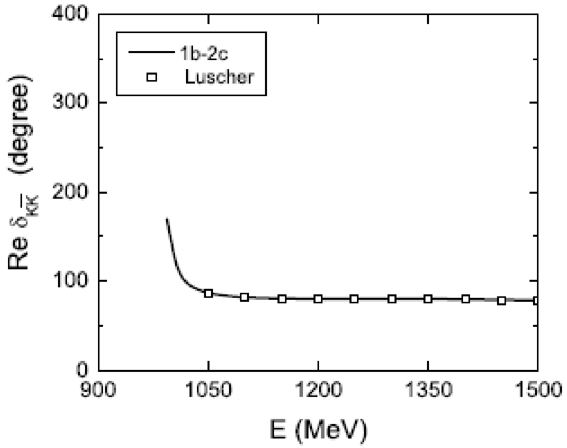

Below the threshold of $\bar{K}K$

$$L \text{ —— } E \text{ —— } \delta_{\pi\pi}(E)$$

$$\delta_{\pi\pi}(k) = \Delta_{\pi\pi}(L) \bmod \pi$$

M. Luscher, NPB 354, 531 (1991).

$$\Delta_\alpha(L) = \tan^{-1}\left(\frac{q_\alpha \pi^{3/2}}{Z_{00}(1, q_\alpha^2)}\right)$$

$$q_\alpha = \sqrt{\frac{E(L)^2}{4} - m_\alpha^2}$$

How to use **Lüscher's Method** ?

ππ –> ππ & ππ –> $\bar{K}$K & $\bar{K}$K–> $\bar{K}$K

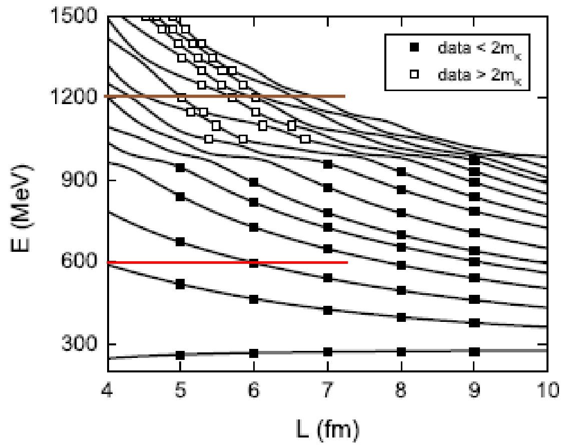

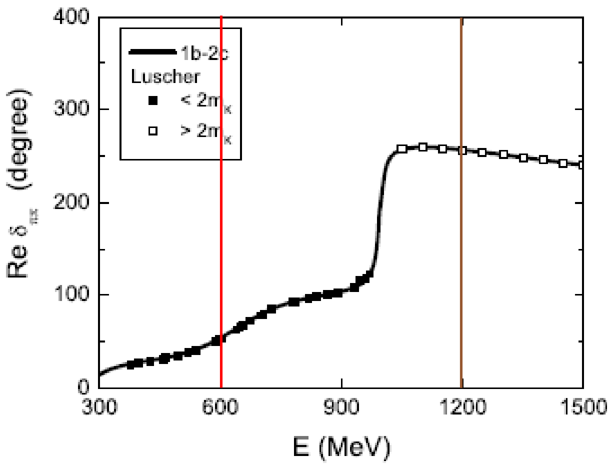

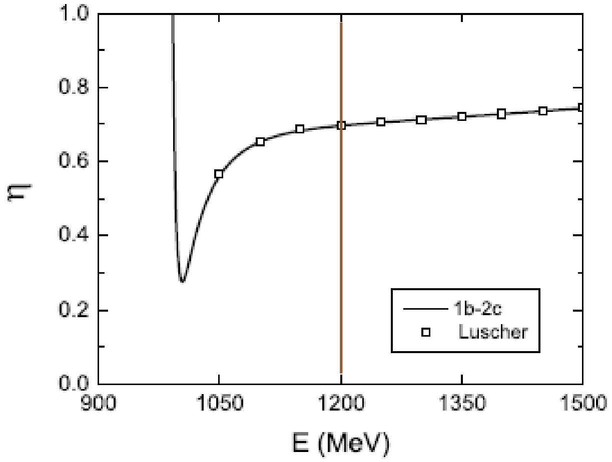

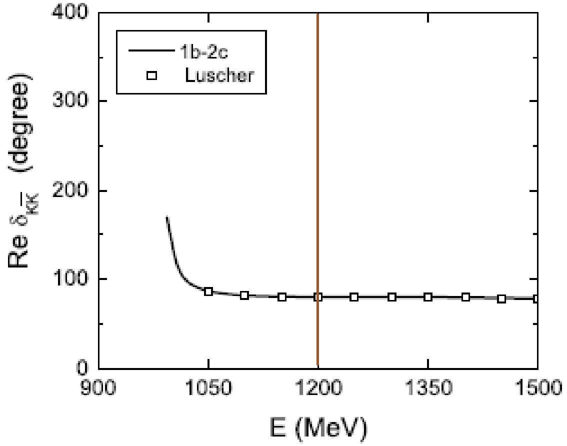

Below the threshold of $\bar{K}$K

L —— E —— $\delta_{\pi\pi}(E)$

$$\delta_{\pi\pi}(k)=\Delta_{\pi\pi}(L)\ \mathrm{mod}\ \pi$$

M. Luscher, NPB 354, 531 (1991).

Above the threshold of $\bar{K}$K

L$_1$, L$_2$, L$_3$ —— E

$$\Delta_\alpha(L)=\tan^{-1}\left(\frac{q_\alpha \pi^{3/2}}{Z_{00}(1,q_\alpha^2)}\right)$$

$$q_\alpha=\sqrt{\frac{E(L)^2}{4}-m_\alpha^2}$$

⇕

$\delta_{\pi\pi}(E)$, $\delta_{K\bar{K}}(E)$, $\eta(E)$

$$0=\cos\left(\Delta_{\pi\pi}(L)+\Delta_{K\bar{K}}(L)-\delta_{\pi\pi}(E)-\delta_{K\bar{K}}(E)\right)$$
$$-\eta\cos\left(\Delta_{\pi\pi}(L)-\Delta_{K\bar{K}}(L)-\delta_{\pi\pi}(E)+\delta_{K\bar{K}}(E)\right)$$

S. He, X. Feng, and C. Liu, JHEP 07(2005)011

Resonance

(Mass , Width, Pole position, Coupling)

Lattice QCD

T matrix
(Phase Shifts, inelasticity)

Lüscher's Method

M. Luscher, NPB 354, 531 (1991).

Lattice Spectrum

Partial Wave Analysis

Lattice QCD

Non-perturbative

Experimental Observable
(Differential Cross Sections)

QCD theory

1. QCD theory: on a box in the Euclid four space

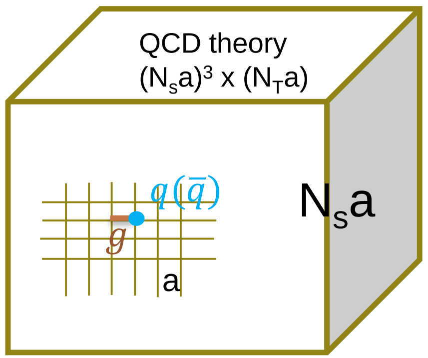

2. a -> UV cutoff, $N_s a$ -> Infrared truncation
3. Lattice QCD -> a model of statistical physics.

$$\langle O \rangle = \int D\phi O[\phi] P[\phi] \qquad P[\phi] = \frac{1}{Z} e^{-S[\phi]} \qquad Z = \int D\phi e^{-S[\phi]}$$

Φ: field quantity, *S*[*ϕ*]: Action, *O*[*ϕ*]:physical quantity

4. Monte Carlo method
5. Three steps for Lattice QCD to real world

a, Configuration

b, Measurement $\sum_{(\vec{y}-\vec{x})\in Z^3} e^{i\vec{p}.(\vec{y}-\vec{x})} \langle T(\psi(t;\vec{y}), \psi^\dagger(t;\vec{y})) \rangle \sim \sum_{\Gamma,i} Z_i^\Gamma e^{-E_i^\Gamma t}$

c, Transformation

Resonance

(Mass , Width, Pole position, Coupling)

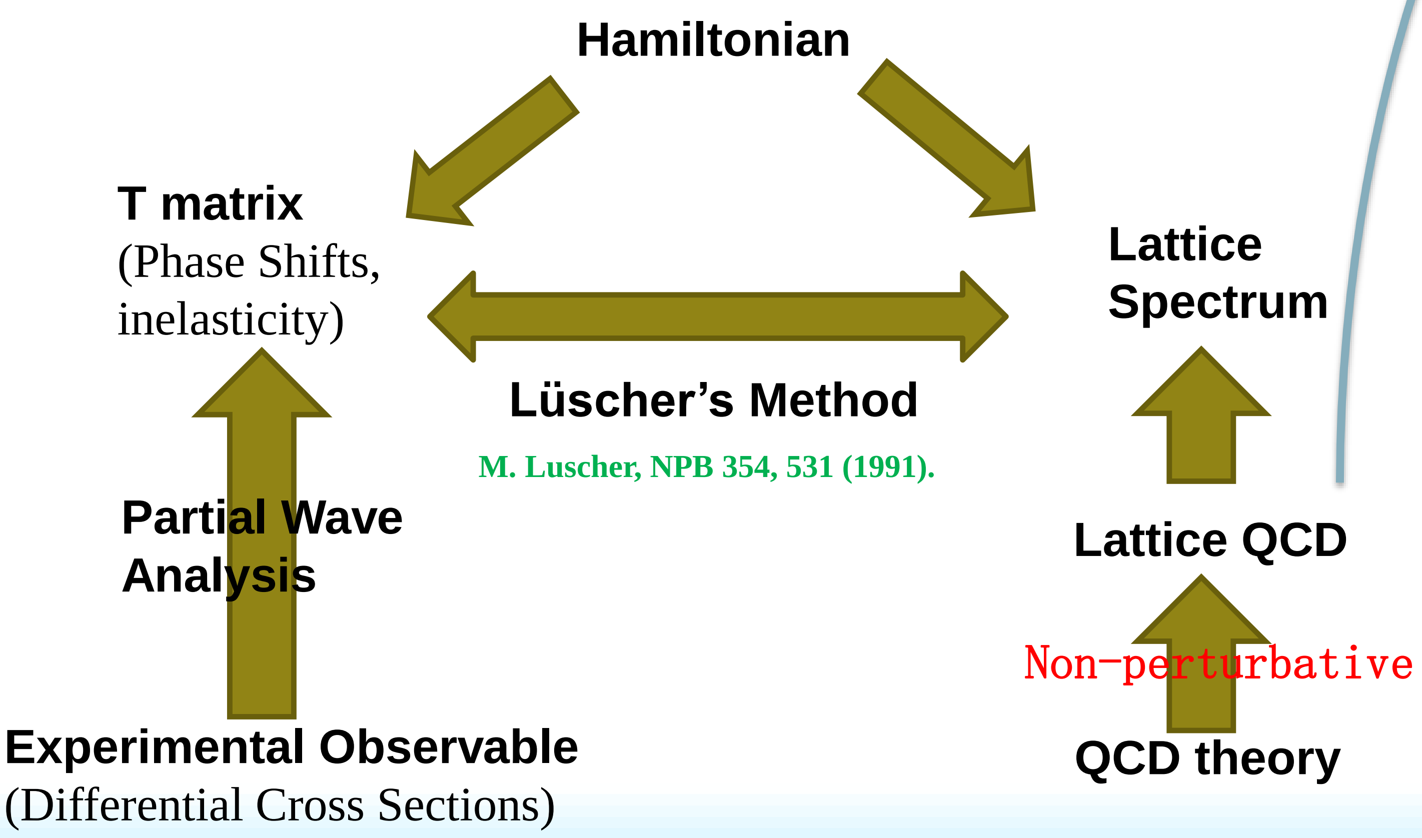

Lattice QCD

1. QCD theory: on a box in the Euclid four space

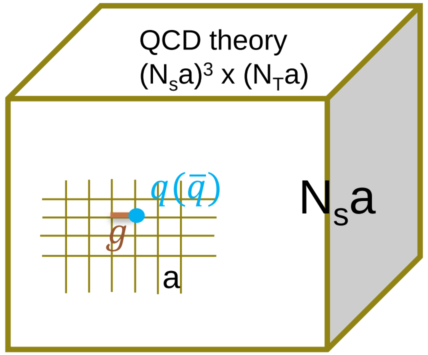

2. a -> UV cutoff, $N_s a$ -> Infrared truncation
3. Lattice QCD -> a model of statistical physics.

$$\langle O \rangle = \int D\phi O[\phi] P[\phi] \qquad P[\phi] = \frac{1}{Z} e^{-S[\phi]} \qquad Z = \int D\phi e^{-S[\phi]}$$

Φ: field quantity, *S*[*ϕ*]: Action, *O*[*ϕ*]:physical quantity

4. Monte Carlo method
5. Three steps for Lattice QCD to real world

a, Configuration

b, Measurement $\sum_{(\vec{y}-\vec{x})\in Z^3} e^{i\vec{p}\cdot(\vec{y}-\vec{x})} \left\langle T\left(\psi(t;\vec{y}), \psi^\dagger(t;\vec{y})\right)\right\rangle \sim \sum_{\Gamma,i} Z_i^\Gamma e^{-E_i^\Gamma t}$

c, Transformation

Resonance

(Mass , Width, Pole position, Coupling)

J. M. M. Hall etc. PRD 87(2013), 094510
J.-j. Wu etc. PRC90 (2014), 055206
Y. Li etc. PRD 101(2020), 114501
PRD 103(2021), 094518

Hamiltonian

T matrix
(Phase Shifts, inelasticity)

Same Quality

Lattice Spectrum

Lüscher's Method

M. Luscher, NPB 354, 531 (1991).

Partial Wave Analysis

Lattice QCD

Non-perturbative

Experimental Observable
(Differential Cross Sections)

QCD theory

Lattice QCD

1. QCD theory: on a box in the Euclid four space

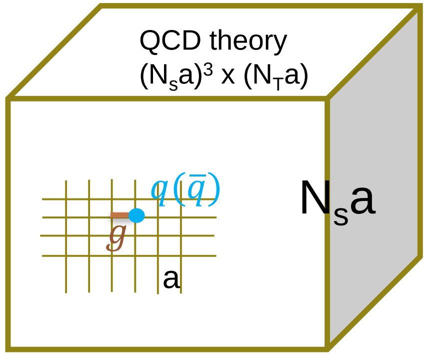

2. a -> UV cutoff, $N_s a$ -> Infrared truncation
3. Lattice QCD -> a model of statistical physics.

$$\langle O \rangle = \int D\phi O[\phi] P[\phi] \qquad P[\phi] = \frac{1}{Z} e^{-S[\phi]} \qquad Z = \int D\phi e^{-S[\phi]}$$

Φ: field quantity, *S*[*ϕ*]: Action, *O*[*ϕ*]:physical quantity

4. Monte Carlo method
5. Three steps for Lattice QCD to real world

a, Configuration

b, Measurement $\sum_{(\vec{y}-\vec{x})\in Z^3} e^{i\vec{p}.(\vec{y}-\vec{x})} \left\langle T\left(\psi(t;\vec{y}), \psi^\dagger(t;\vec{y})\right)\right\rangle \sim \sum_{\Gamma,i} Z_i^\Gamma e^{-E_i^\Gamma t}$

c, Transformation

Resonance

(Mass , Width, Pole position, Coupling)

J. M. M. Hall etc. PRD 87(2013), 094510
J.-j. Wu etc. PRC90 (2014), 055206
Y. Li etc. PRD 101(2020), 114501
PRD 103(2021), 094518

Hamiltonian

T matrix
(Phase Shifts, inelasticity)

Same Quality

Lattice Spectrum

Lüscher's Method

M. Luscher, NPB 354, 531 (1991).

Partial Wave Analysis

Lattice QCD

Non-perturbative

Experimental Observable
(Differential Cross Sections)

QCD theory

Lattice QCD

1. QCD theory: on a box in the Euclid four space

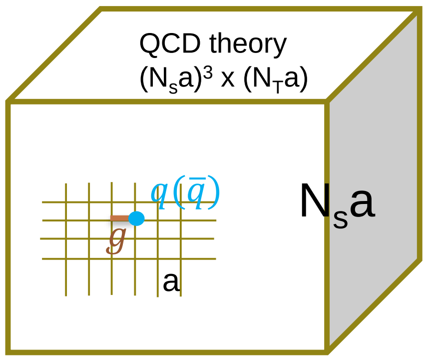

2. a -> UV cutoff, $N_s a$ -> Infrared truncation
3. Lattice QCD -> a model of statistical physics.

$$\langle O \rangle = \int D\phi O[\phi] P[\phi] \qquad P[\phi] = \frac{1}{Z} e^{-S[\phi]} \qquad Z = \int D\phi e^{-S[\phi]}$$

Φ: field quantity, *S*[*ϕ*]: Action, *O*[*ϕ*]:physical quantity

4. Monte Carlo method
5. Three steps for Lattice QCD to real world

a, Configuration

b, Measurement $\sum_{(\vec{y}-\vec{x})\in Z^3} e^{i\vec{p}\cdot(\vec{y}-\vec{x})} \langle T(\psi(t;\vec{y}),\psi^\dagger(t;\vec{y}))\rangle \sim \sum_{\Gamma,i} Z_i^\Gamma e^{-E_i^\Gamma t}$

c, Transformation

Introduction of HEFT

1. **Finite-volume matrix Hamiltonian model for a Δ→Nπ system**
   J.M.M. Hall, A.C.-P. Hsu, D.B. Leinweber, A.W.Thomas, R.D. Young Phys.Rev. D87 (2013) no.9, 094510
2. **Finite-volume Hamiltonian method for coupled-channels interactions in lattice QCD**
   Jia-Jun Wu, T.-S.H.Lee, A.W.Thomas, R.D. Young Phys.Rev. C90 (2014) no.5, 055206
3. **Hamiltonian effective field theory study of the N∗(1535) resonance in lattice QCD**
   Zhan-Wei Liu, Waseem Kamleh, Derek B. Leinweber, Finn M. Stokes, Anthony W. Thomas, Jia-Jun Wu
   Phys.Rev.Lett. 116 (2016) no.8, 082004
4. **Lattice QCD Evidence that the Λ(1405) Resonance is an Antikaon-Nucleon Molecule**
   J.M.M. Hall, Waseem Kamleh, Derek B. Leinweber, Benjamin J. Menadue, Benjamin J. Owen, A.W.Thomas, R.D. Young
   Phys.Rev.Lett. 114 (2015) no.13, 132002
5. **Hamiltonian effective field theory study of the N∗(1440) resonance in lattice QCD**
   Zhan-Wei Liu, Waseem Kamleh, Derek B. Leinweber, Finn M. Stokes, Anthony W. Thomas, Jia-Jun Wu
   Phys.Rev. D95 (2017) no.3, 034034
6. **Structure of the Λ(1405) from Hamiltonian effective field theory**
   Zhan-Wei Liu, Jonathan M.M. Hall, Derek B. Leinweber, Anthony W. Thomas, Jia-Jun Wu
   Phys.Rev. D95 (2017) no.1, 014506
7. **Nucleon resonance structure in the finite volume of lattice QCD**
   Jia-jun Wu, H. Kamano, T.-S.H.Lee , Derek B. Leinweber, Anthony W. Thomas Phys.Rev. D95 (2017) no.11, 114507
8. **Structure of the Roper Resonance from Lattice QCD Constraints**
   Jia-jun Wu, Derek B. Leinweber, Zhan-wei Liu, Anthony W.Thomas Phys.Rev. D97(2018) no.9, 094509
9. **Kaonic Hydrogen and Deuterium in Hamiltonian Effective Field Theory**
   Zhan-wei Liu, Jia-jun Wu, Derek B. Leinweber, Anthony W. Thomas Phys.Lett.B 808(2020),135652
10. **Partial Wave Mixing in Hamiltonian Effective Field Theory**
    Yan Li, Jia-jun Wu, Curtis D. Abell, Derek B. Leinweber, Anthony W. Thomas Phys.Rev. D101(2020) no.11,114501
11. **Hamiltonian effective field theory in elongated or moving finite volume**
    Yan Li, Jia-jun Wu, Derek B. Leinweber, Anthony W. Thomas Phys.Rev. D103(2021) no.9, 094518
12. **Regularisation in Nonperturbative Extensions of Effective Field Theory**
    Curtis D. Abell, Derek B. Leinweber, Anthony W. Thomas, Jia-jun Wu arXiv: 2110.14113
13. **Novel Coupled Channel Framework Connecting the Quark Model and Lattice QCD for the Near-threshold Ds States** Zhi Yang, Guang-Juan Wang, Jia-jun Wu, Shi-lin Zhu, Makoto Oka Phys.Rev.Lett.128(2022),112001
14. **The investigations of the P-wave B_s states combining quark model and lattice QCD in the coupled channel framework** Zhi Yang, Guang-Juan Wang, Jia-jun Wu, Shi-lin Zhu, Makoto Oka arXiv: 2207.07320

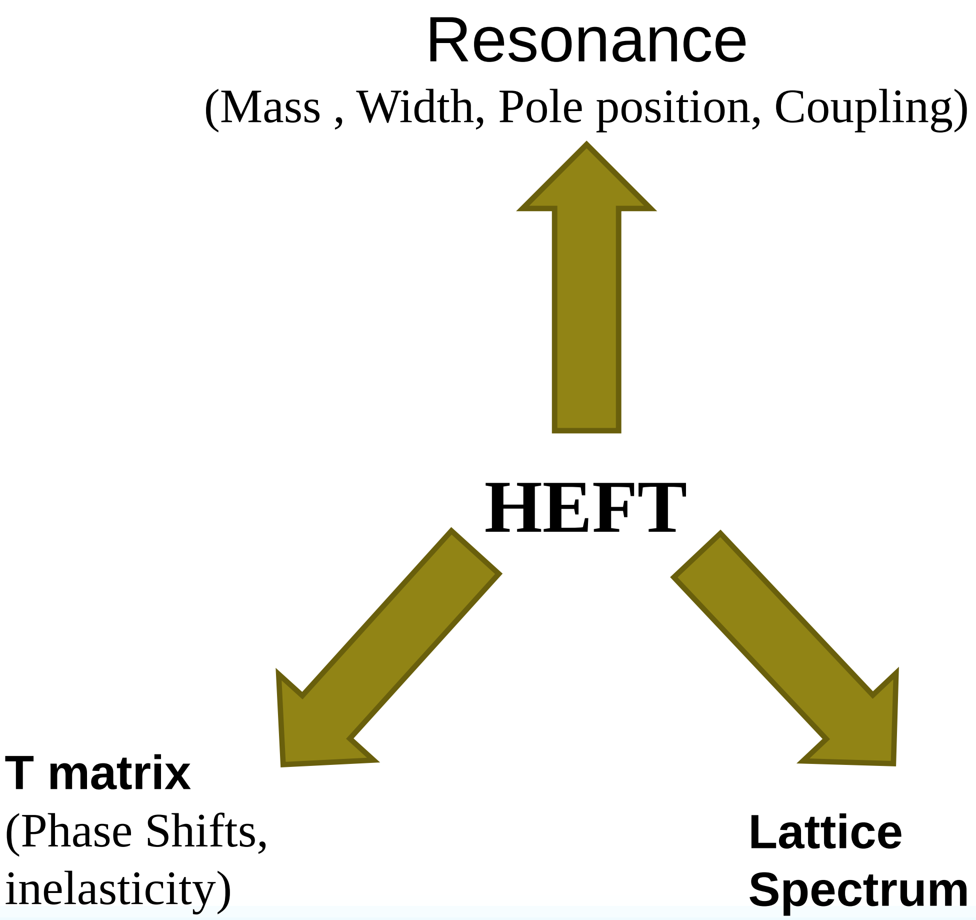

Introduction of HEFT

J. M. M. Hall etc. PRD 87(2013), 094510
J.-j. Wu etc. PRC90 (2014), 055206
Y. Li etc. PRD 101(2020), 114501
PRD 103(2021), 094518

$$H = H_0 + H_I$$

$$H_0 = \sum_{i=1,n} |B_i\rangle m_i \langle B_i| + \sum_{\alpha} |\alpha(k_\alpha)\rangle \left[\sqrt{m_{\alpha 1}^2 + k_\alpha^2} + \sqrt{m_{\alpha 2}^2 + k_\alpha^2}\right] \langle \alpha(k_\alpha)|$$

$|B_i>$ bare state， bare mass m_i

$|\alpha(k_\alpha)>$ non-interaction channels

$$H_I = \hat{g} + \hat{v}$$

$$\hat{g} = \sum_{\alpha} \sum_{i=1,n} \left[|\alpha(k_\alpha)\rangle g_{i,\alpha}^{+} \langle B_i| + |B_i\rangle g_{i,\alpha} \langle \alpha(k_\alpha)| \right]$$

$$\hat{v} = \sum_{\alpha,\beta} |\alpha(k_\alpha)\rangle v_{\alpha,\beta} \langle \beta(k_\beta)|$$

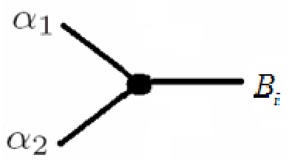

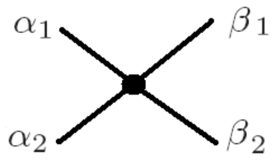

Resonance
(Mass , Width, Pole position, Coupling)

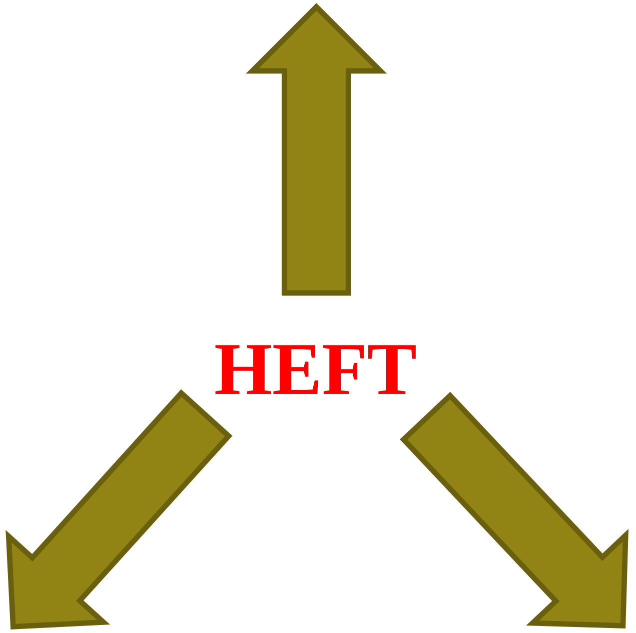

T matrix
(Phase Shifts, inelasticity)

Lattice Spectrum

Introduction of HEFT

Argonne-Osaka Model

- **T Matrix:**

$$t_{\alpha,\beta}(k_\alpha,k_\beta,E)=V_{\alpha,\beta}(k_\alpha,k_\beta)+\sum_\gamma\int k_\gamma{}^2dk_\gamma\,\frac{V_{\alpha,\gamma}(k_\alpha,k_\gamma)t_{\gamma,\beta}(k_\gamma,k_\beta,E)}{E-\sqrt{m_{\gamma 1}^2+k_\gamma^2}-\sqrt{m_{\gamma 2}^2+k_\gamma^2}+i\varepsilon}$$

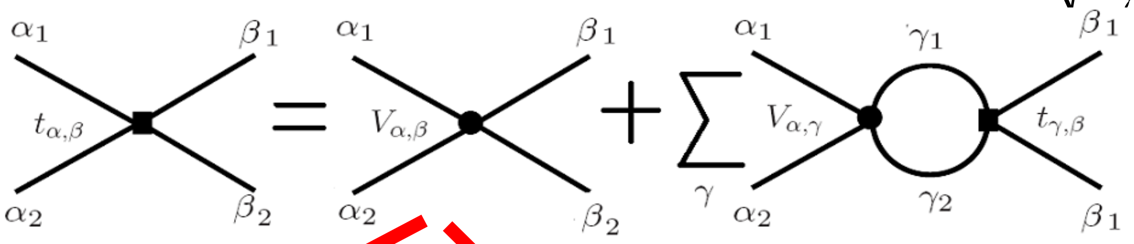

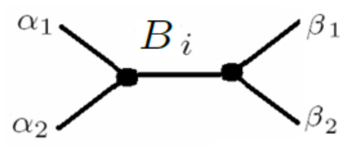

$$g^*_{i,\alpha}\frac{1}{E-m_i}g_{i,\beta}$$

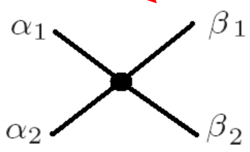

$$v_{\alpha,\beta}$$

$$S_{\alpha,\beta}=1-i2\sqrt{\rho_\alpha}\,t_{\alpha,\beta}(k_{0\alpha},k_{0\beta},E)\sqrt{\rho_\beta}$$

$$\rho_\alpha=\frac{\pi k_{0\alpha}\sqrt{m_{\alpha 1}^2+k_{0\alpha}^2}\sqrt{m_{\alpha 1}^2+k_{0\alpha}^2}}{E}$$

$$\eta e^{2i\delta_\alpha}=S_{\alpha,\alpha}$$

Resonance

(Mass , Width, Pole position, Coupling)

HEFT

T matrix

(Phase Shifts, inelasticity)

Lattice Spectrum

Introduction of HEFT

J.-j. Wu etc. PRC90 (2014), 055206

- **Hamiltonian with discrete momentum**

Continuous → Discrete

Continuous			
$\int d\vec{k}$	and $\left\|\alpha(\vec{k}_\alpha)\right\rangle$	and	$\left\langle\beta(\vec{k}_\beta)\middle\|\alpha(\vec{k}_\alpha)\right\rangle = \delta_{\alpha\beta}\delta(\vec{k}_\alpha - \vec{k}_\beta)$
↓	↓		↓
$\sum_i \left(\frac{2\pi}{L}\right)^3$	and $\left(\frac{2\pi}{L}\right)^{-3/2}\left\|\vec{k}_i,-\vec{k}_i\right\rangle_\alpha$	and	${}_\beta\left\langle\vec{k}_j,-\vec{k}_j\middle\|\vec{k}_i,-\vec{k}_i\right\rangle_\alpha = \delta_{\alpha\beta}\delta_{ij}$

$$H_0 = \sum_{i=1,n}\left|B_i\right\rangle m_i \left\langle B_i\right| + \sum_{\alpha,i}\left|\vec{k}_i,-\vec{k}_i\right\rangle_\alpha \left[\sqrt{m^2_{\alpha_B}+k^2_\alpha}+\sqrt{m^2_{\alpha_M}+k^2_\alpha}\right]_\alpha \left\langle\vec{k}_i,-\vec{k}_i\right|$$

$$H_I = \sum_j \left(\frac{2\pi}{L}\right)^{3/2}\sum_\alpha\sum_{i=1,n}\left[\left|\vec{k}_j,-\vec{k}_j\right\rangle_\alpha g^+_{i,\alpha}\left\langle B_i\right| + \left|B_i\right\rangle g_{i,\alpha}\ {}_\alpha\left\langle\vec{k}_j,-\vec{k}_j\right|\right] + \sum_{i,j}\left(\frac{2\pi}{L}\right)^3\sum_{\alpha,\beta}\left|\vec{k}_i,-\vec{k}_i\right\rangle_\alpha v_{\alpha,\beta}\ {}_\beta\left\langle\vec{k}_j,-\vec{k}_j\right|$$

$$[H_0]_{N_c+1} = \begin{pmatrix} m_0 & 0 & 0 & \cdots & 0 & 0 & \cdots \\ 0 & \epsilon_1(k_0) & 0 & \cdots & 0 & 0 & \cdots \\ 0 & 0 & \epsilon_2(k_0) & \cdots & 0 & 0 & \cdots \\ 0 & 0 & 0 & \ddots & 0 & 0 & \cdots \\ 0 & 0 & 0 & \cdots & \epsilon_{n_c}(k_0) & 0 & \cdots \\ 0 & 0 & 0 & \cdots & 0 & \epsilon_1(k_1) & \cdots \\ \vdots & \vdots & \vdots & \vdots & \vdots & \vdots & \ddots \end{pmatrix}$$

$$[H_I]_{N_c+1} = \begin{pmatrix} 0 & g_1^V(k_0) & g_2^V(k_0) & \cdots & g_{n_c}^V(k_0) & g_1^V(k_1) & \cdots \\ g_1^V(k_0) & v_{1,1}^V(k_0,k_0) & v_{1,2}^V(k_0,k_0) & \cdots & v_{1,n_c}^V(k_0,k_0) & v_{1,1}^V(k_0,k_1) & \cdots \\ g_2^V(k_0) & v_{2,1}^V(k_0,k_0) & v_{2,2}^V(k_0,k_0) & \cdots & v_{2,n_c}^V(k_0,k_0) & v_{2,1}^V(k_0,k_1) & \cdots \\ \vdots & \vdots & \vdots & \ddots & \vdots & \vdots & \cdots \\ g_{n_c}^V(k_0) & v_{n_c,1}^V(k_0,k_0) & v_{n_c,2}^V(k_0,k_0) & \cdots & v_{n_c,n_c}^V(k_0,k_0) & v_{n_c,1}^V(k_0,k_1) & \cdots \\ g_1^V(k_1) & v_{1,1}^V(k_1,k_0) & v_{1,2}^V(k_1,k_0) & \cdots & v_{1,n_c}^V(k_1,k_0) & v_{1,1}^V(k_1,k_1) & \cdots \\ \vdots & \vdots & \vdots & \vdots & \vdots & \vdots & \ddots \end{pmatrix}$$

$$(H_0+H_I)\,|\Psi> = E\,|\Psi>$$

Eigen-Value ⟷ Lattice Spectrum

Eigen-Vector

Resonance
(Mass , Width, Pole position, Coupling)

HEFT

T matrix
(Phase Shifts, inelasticity)

Lattice Spectrum

Introduction of HEFT

Y. Li etc. PRD 101(2020), 114501
PRD 103(2021), 094518

- **Partial Wave Mixing, Moving system, Elongated volume**

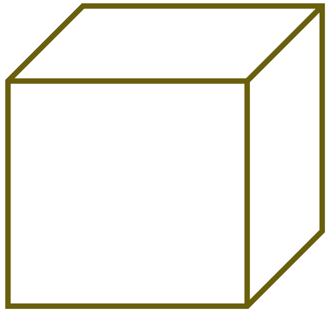

O_h

$A_1^{\pm}$, $A_2^{\pm}$, $E^{\pm}$, $T_1^{\pm}$, $T_2^{\pm}$

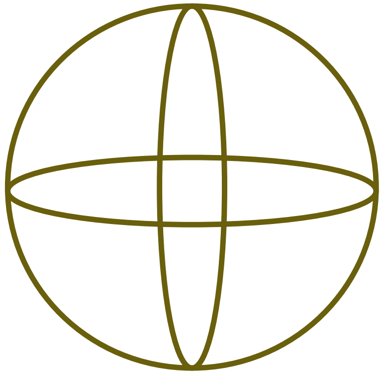

O(3)

$L^p = 0^+,\ 1^-,\ 2^+,$ ……

O_h	O(3)
A_1^+	0^+ , 4^+ , ….
E^+	2^+ , 4^+ , ….
T_1^+	4^+ , ….
T_2^+	2^+ , 4^+ , ….
A_2^-	3^- , 7^- , $9-$, ….
T_1^-	1^- , 3^- , ….
T_2^-	3^- , ….

$$[P_N]_{l',m';l,m} := 4\pi \sum_{|\mathbf{n}|^2=N} Y^*_{l'm'}(\hat{\mathbf{n}}) Y_{lm}(\hat{\mathbf{n}})$$

Resonance

(Mass , Width, Pole position, Coupling)

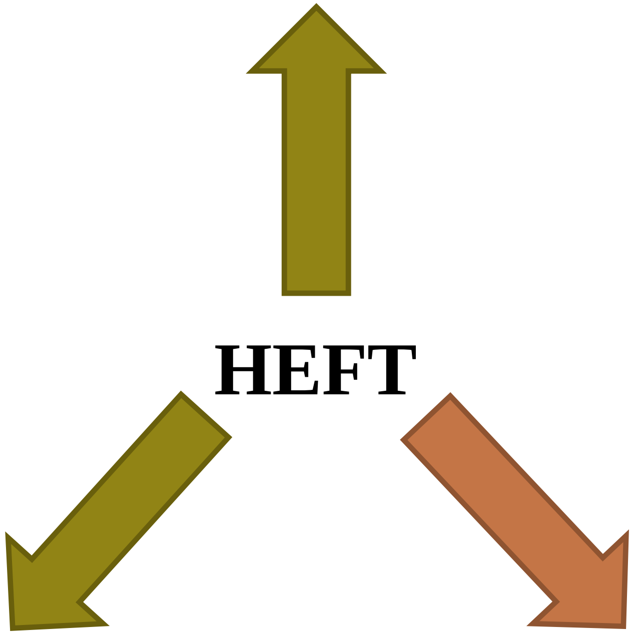

HEFT

T matrix
(Phase Shifts, inelasticity)

Lattice Spectrum

Introduction of HEFT

Y. Li etc. PRD 101(2020), 114501
PRD 103(2021), 094518

- **Partial Wave Mixing, Moving system, Elongated volume**

s-wave | p-wave | d-wave | f-wave | g-wave

$$
\begin{pmatrix}
1.00 & 0 & 0 & 0 & 0 & 0 & 0 & 0 & 0 & 0 & 0 & 0 & 0 & 0 & 0 & 0 & 1.05 & 0 & 0 & 0 & 1.75 & 0 & 0 & 0 & 1.05 \\
0 & 1.00 & 0 & 0 & 0 & 0 & 0 & 0 & 0 & 0 & 0 & -0.94 & 0 & 0 & 0 & -1.21 & 0 & 0 & 0 & 0 & 0 & 0 & 0 & 0 & 0 \\
0 & 0 & 1.00 & 0 & 0 & 0 & 0 & 0 & 0 & 0 & 0 & 0 & 1.53 & 0 & 0 & 0 & 0 & 0 & 0 & 0 & 0 & 0 & 0 & 0 & 0 \\
0 & 0 & 0 & 1.00 & 0 & 0 & 0 & 0 & 0 & -1.21 & 0 & 0 & 0 & -0.94 & 0 & 0 & 0 & 0 & 0 & 0 & 0 & 0 & 0 & 0 & 0 \\
0 & 0 & 0 & 0 & 1.25 & 0 & 0 & 0 & 1.25 & 0 & 0 & 0 & 0 & 0 & 0 & 0 & 0 & 0 & -1.08 & 0 & 0 & 0 & -1.08 & 0 & 0 \\
0 & 0 & 0 & 0 & 0 & 0 & 0 & 0 & 0 & 0 & 0 & 0 & 0 & 0 & 0 & 0 & 0 & 0 & 0 & 0 & 0 & 0 & 0 & 0 & 0 \\
0 & 0 & 0 & 0 & 0 & 0 & 2.50 & 0 & 0 & 0 & 0 & 0 & 0 & 0 & 0 & 0 & -1.17 & 0 & 0 & 0 & 1.40 & 0 & 0 & 0 & -1.17 \\
0 & 0 & 0 & 0 & 0 & 0 & 0 & 0 & 0 & 0 & 0 & 0 & 0 & 0 & 0 & 0 & 0 & 0 & 0 & 0 & 0 & 0 & 0 & 0 & 0 \\
0 & 0 & 0 & 0 & 1.25 & 0 & 0 & 0 & 1.25 & 0 & 0 & 0 & 0 & 0 & 0 & 0 & 0 & 0 & -1.08 & 0 & 0 & 0 & -1.08 & 0 & 0 \\
0 & 0 & 0 & -1.21 & 0 & 0 & 0 & 0 & 0 & 1.46 & 0 & 0 & 0 & 1.13 & 0 & 0 & 0 & 0 & 0 & 0 & 0 & 0 & 0 & 0 & 0 \\
0 & 0 & 0 & 0 & 0 & 0 & 0 & 0 & 0 & 0 & 0 & 0 & 0 & 0 & 0 & 0 & 0 & 0 & 0 & 0 & 0 & 0 & 0 & 0 & 0 \\
0 & -0.94 & 0 & 0 & 0 & 0 & 0 & 0 & 0 & 0 & 0 & 0.88 & 0 & 0 & 0 & 1.13 & 0 & 0 & 0 & 0 & 0 & 0 & 0 & 0 & 0 \\
0 & 0 & 1.53 & 0 & 0 & 0 & 0 & 0 & 0 & 0 & 0 & 0 & 2.33 & 0 & 0 & 0 & 0 & 0 & 0 & 0 & 0 & 0 & 0 & 0 & 0 \\
0 & 0 & 0 & -0.94 & 0 & 0 & 0 & 0 & 0 & 1.13 & 0 & 0 & 0 & 0.88 & 0 & 0 & 0 & 0 & 0 & 0 & 0 & 0 & 0 & 0 & 0 \\
0 & 0 & 0 & 0 & 0 & 0 & 0 & 0 & 0 & 0 & 0 & 0 & 0 & 0 & 0 & 0 & 0 & 0 & 0 & 0 & 0 & 0 & 0 & 0 & 0 \\
0 & -1.21 & 0 & 0 & 0 & 0 & 0 & 0 & 0 & 0 & 0 & 1.13 & 0 & 0 & 0 & 1.46 & 0 & 0 & 0 & 0 & 0 & 0 & 0 & 0 & 0 \\
1.05 & 0 & 0 & 0 & 0 & 0 & -1.17 & 0 & 0 & 0 & 0 & 0 & 0 & 0 & 0 & 0 & 1.64 & 0 & 0 & 0 & 1.18 & 0 & 0 & 0 & 1.64 \\
0 & 0 & 0 & 0 & 0 & 0 & 0 & 0 & 0 & 0 & 0 & 0 & 0 & 0 & 0 & 0 & 0 & 0 & 0 & 0 & 0 & 0 & 0 & 0 & 0 \\
0 & 0 & 0 & 0 & -1.08 & 0 & 0 & 0 & -1.08 & 0 & 0 & 0 & 0 & 0 & 0 & 0 & 0 & 0 & 0.94 & 0 & 0 & 0 & 0.94 & 0 & 0 \\
0 & 0 & 0 & 0 & 0 & 0 & 0 & 0 & 0 & 0 & 0 & 0 & 0 & 0 & 0 & 0 & 0 & 0 & 0 & 0 & 0 & 0 & 0 & 0 & 0 \\
1.75 & 0 & 0 & 0 & 0 & 0 & 1.40 & 0 & 0 & 0 & 0 & 0 & 0 & 0 & 0 & 0 & 1.18 & 0 & 0 & 0 & 3.84 & 0 & 0 & 0 & 1.18 \\
0 & 0 & 0 & 0 & 0 & 0 & 0 & 0 & 0 & 0 & 0 & 0 & 0 & 0 & 0 & 0 & 0 & 0 & 0 & 0 & 0 & 0 & 0 & 0 & 0 \\
0 & 0 & 0 & 0 & -1.08 & 0 & 0 & 0 & -1.08 & 0 & 0 & 0 & 0 & 0 & 0 & 0 & 0 & 0 & 0.94 & 0 & 0 & 0 & 0.94 & 0 & 0 \\
0 & 0 & 0 & 0 & 0 & 0 & 0 & 0 & 0 & 0 & 0 & 0 & 0 & 0 & 0 & 0 & 0 & 0 & 0 & 0 & 0 & 0 & 0 & 0 & 0 \\
1.05 & 0 & 0 & 0 & 0 & 0 & -1.17 & 0 & 0 & 0 & 0 & 0 & 0 & 0 & 0 & 0 & 1.64 & 0 & 0 & 0 & 1.18 & 0 & 0 & 0 & 1.64
\end{pmatrix}
$$

$$[P_{N=1}] \big/ C_3(1) \qquad C_3(1) = 6$$

$$[P_N]_{l',m';l,m} := \langle N; l', m' | N; l, m \rangle = 4\pi \sum_{|\mathbf{n}|^2 = N} Y^*_{l'm'}(\hat{\mathbf{n}}) Y_{lm}(\hat{\mathbf{n}})$$

25×25 matrix ordered as $(l, m) = (0,0), (1,-1), (1,0), (1,1), \cdots, (4,4)$

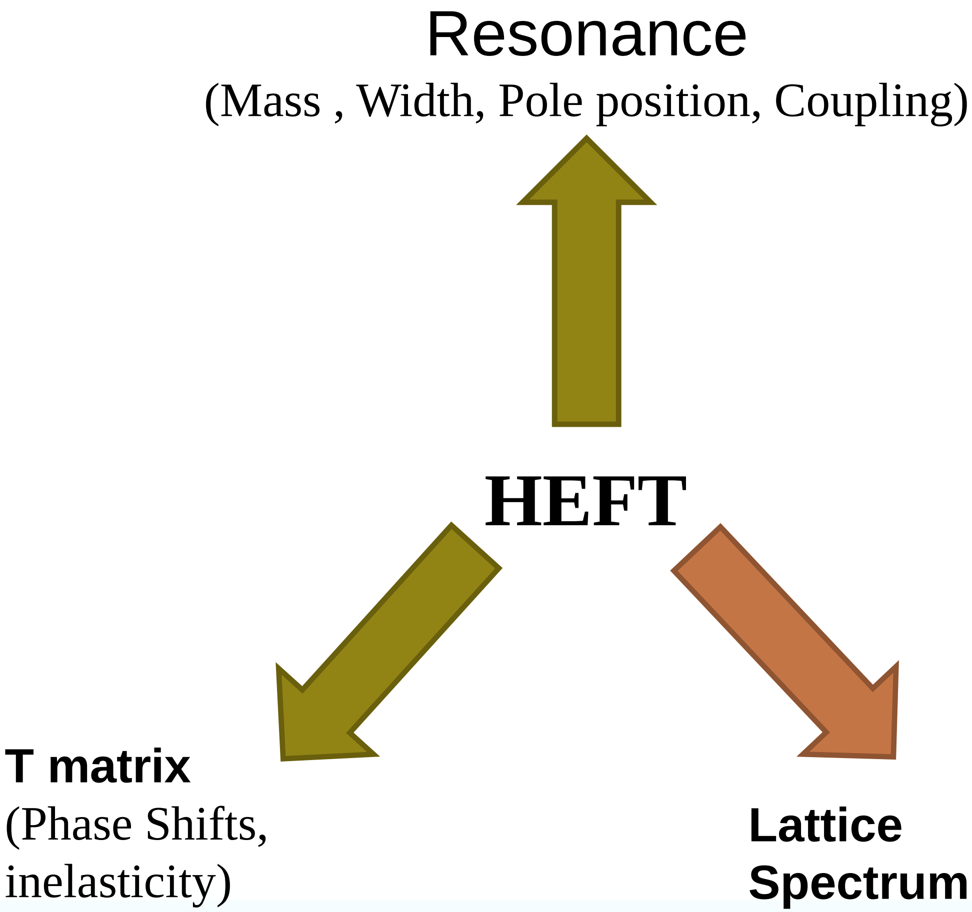

Introduction of HEFT

Y. Li etc. PRD 101(2020), 114501
PRD 103(2021), 094518

- **Partial Wave Mixing, Moving system, Elongated volume**

s-wave	p-wave			d-wave					f-wave							g-wave								
1.00	0	0	0	0	0	0	0	0	0	0	0	0	0	0	0	0.07	0	0	0	0.11	0	0	0	0.07
0	1.00	0	0	0	0	0	0	0	0	0	−0.06	0	0	0	−0.08	0	0	0	0	0	0	0	0	0
0	0	1.00	0	0	0	0	0	0	0	0	0	0.10	0	0	0	0	0	0	0	0	0	0	0	0
0	0	0	1.00	0	0	0	0	0	−0.08	0	0	0	−0.06	0	0	0	0	0	0	0	0	0	0	0
0	0	0	0	1.02	0	0	0	0.08	0	0	0	0	0	0	0	0	0	−0.07	0	0	0	−0.09	0	0
0	0	0	0	0	0.94	0	0	0	0	0	0	0	0	0	0	0	0	0	−0.01	0	0	0	0.03	0
0	0	0	0	0	0	1.10	0	0	0	0	0	0	0	0	0	−0.09	0	0	0	0.10	0	0	0	−0.09
0	0	0	0	0	0	0	0.94	0	0	0	0	0	0	0	0	0	0.03	0	0	0	−0.01	0	0	0
0	0	0	0	0.08	0	0	0	1.02	0	0	0	0	0	0	0	0	0	−0.09	0	0	0	−0.07	0	0
0	0	0	−0.08	0	0	0	0	0	1.03	0	0	0	0.09	0	0	0	0	0	0	0	0	0	0	0
0	0	0	0	0	0	0	0	0	0	0.94	0	0	0	−0.03	0	0	0	0	0	0	0	0	0	0
0	−0.06	0	0	0	0	0	0	0	0	0	0.98	0	0	0	0.09	0	0	0	0	0	0	0	0	0
0	0	0.10	0	0	0	0	0	0	0	0	0	1.10	0	0	0	0	0	0	0	0	0	0	0	0
0	0	0	−0.06	0	0	0	0	0	0.09	0	0	0	0.98	0	0	0	0	0	0	0	0	0	0	0
0	0	0	0	0	0	0	0	0	0	−0.03	0	0	0	0.94	0	0	0	0	0	0	0	0	0	0
0	−0.08	0	0	0	0	0	0	0	0	0	0.09	0	0	0	1.03	0	0	0	0	0	0	0	0	0
0.07	0	0	0	0	0	−0.09	0	0	0	0	0	0	0	0	0	1.04	0	0	0	0.11	0	0	0	0.20
0	0	0	0	0	0	0	0.03	0	0	0	0	0	0	0	0	0	0.93	0	0	0	−0.04	0	0	0
0	0	0	0	−0.07	0	0	0	−0.09	0	0	0	0	0	0	0	0	0	1.03	0	0	0	0.08	0	0
0	0	0	0	0	−0.01	0	0	0	0	0	0	0	0	0	0	0	0	0	0.85	0	0	0	−0.04	0
0.11	0	0	0	0	0	0.10	0	0	0	0	0	0	0	0	0	0.11	0	0	0	1.30	0	0	0	0.11
0	0	0	0	0	0	0	−0.01	0	0	0	0	0	0	0	0	0	−0.04	0	0	0	0.85	0	0	0
0	0	0	0	−0.09	0	0	0	−0.07	0	0	0	0	0	0	0	0	0	0.08	0	0	0	1.03	0	0
0	0	0	0	0	0.03	0	0	0	0	0	0	0	0	0	0	0	0	0	−0.04	0	0	0	0.93	0
0.07	0	0	0	0	0	−0.09	0	0	0	0	0	0	0	0	0	0.20	0	0	0	0.11	0	0	0	1.04

$$[P_{N=581}] \big/ C_3(581) \qquad C_3(581) = 336$$

$$[P_N]_{l',m';l,m} := \langle N; l', m' | N; l, m \rangle = 4\pi \sum_{|\mathbf{n}|^2 = N} Y^*_{l'm'}(\hat{\mathbf{n}}) Y_{lm}(\hat{\mathbf{n}})$$

25×25 matrix ordered as $(l, m) = (0,0), (1,-1), (1,0), (1,1), \cdots, (4,4)$

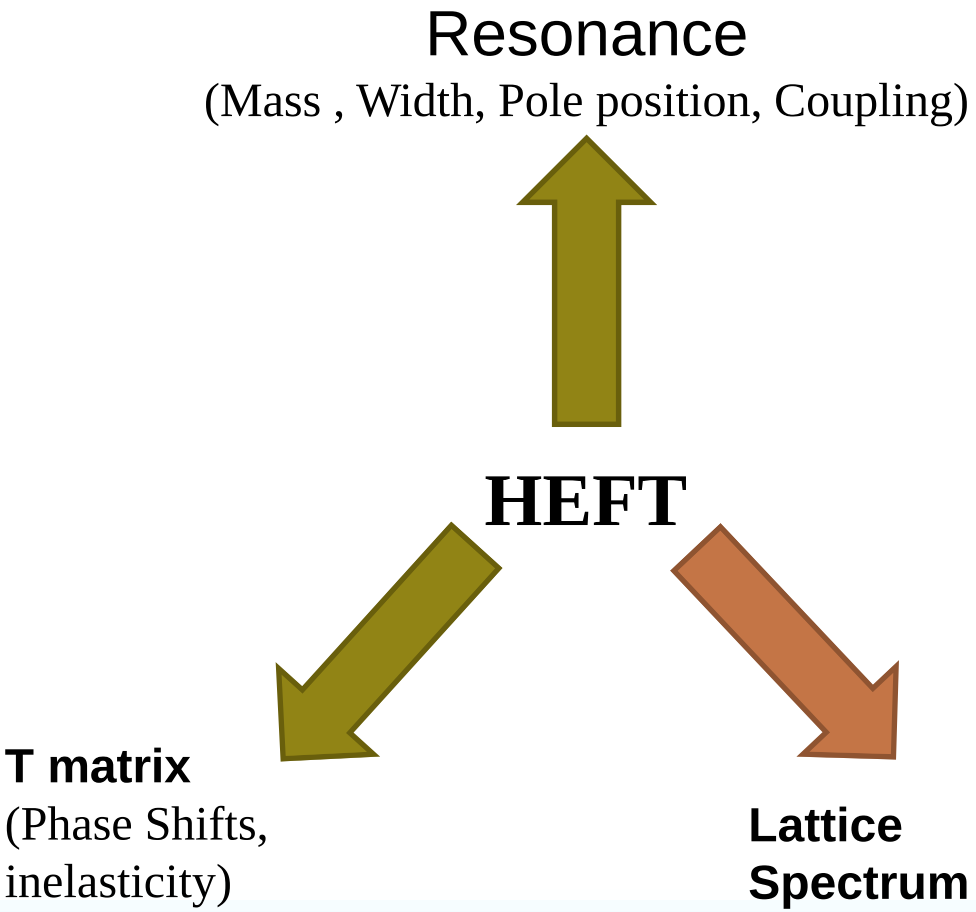

Introduction of HEFT

Y. Li etc. PRD 101(2020), 114501
PRD 103(2021), 094518

- **Partial Wave Mixing, Moving system, Elongated volume**

s-wave | p-wave | d-wave | f-wave | g-wave

$$
\begin{bmatrix}
1.00&0&0&0&0&0&0&0&0&0&0&0&0&0&0&0&-0.01&0&0&0&-0.02&0&0&0&-0.01\\
0&1.00&0&0&0&0&0&0&0&0&0&0.01&0&0&0&0.02&0&0&0&0&0&0&0&0&0\\
0&0&1.00&0&0&0&0&0&0&0&0&0&-0.02&0&0&0&0&0&0&0&0&0&0&0&0\\
0&0&0&1.00&0&0&0&0&0&0.02&0&0&0&0.01&0&0&0&0&0&0&0&0&0&0&0\\
0&0&0&0&1.00&0&0&0&-0.02&0&0&0&0&0&0&0&0&0&0.01&0&0&0&0.02&0&0\\
0&0&0&0&0&1.01&0&0&0&0&0&0&0&0&0&0&0&0&0&0.00&0&0&0&-0.00&0\\
0&0&0&0&0&0&0.98&0&0&0&0&0&0&0&0&0&0.02&0&0&0&-0.02&0&0&0&0.02\\
0&0&0&0&0&0&0&1.01&0&0&0&0&0&0&0&0&0&-0.00&0&0&0&0.00&0&0&0\\
0&0&0&0&-0.02&0&0&0&1.00&0&0&0&0&0&0&0&0&0&0.02&0&0&0&0.01&0&0\\
0&0&0&0.02&0&0&0&0&0&0.99&0&0&0&-0.02&0&0&0&0&0&0&0&0&0&0&0\\
0&0&0&0&0&0&0&0&0&0&1.01&0&0&0&0.00&0&0&0&0&0&0&0&0&0&0\\
0&0.01&0&0&0&0&0&0&0&0&0&1.00&0&0&0&-0.02&0&0&0&0&0&0&0&0&0\\
0&0&-0.02&0&0&0&0&0&0&0&0&0&0.98&0&0&0&0&0&0&0&0&0&0&0&0\\
0&0&0&0.01&0&0&0&0&0&-0.02&0&0&0&1.00&0&0&0&0&0&0&0&0&0&0&0\\
0&0&0&0&0&0&0&0&0&0&0.00&0&0&0&1.01&0&0&0&0&0&0&0&0&0&0\\
0&0.02&0&0&0&0&0&0&0&0&0&-0.02&0&0&0&0.99&0&0&0&0&0&0&0&0&0\\
-0.01&0&0&0&0&0&0.02&0&0&0&0&0&0&0&0&0&0.99&0&0&0&-0.02&0&0&0&-0.03\\
0&0&0&0&0&0&0&-0.00&0&0&0&0&0&0&0&0&0&1.01&0&0&0&0.00&0&0&0\\
0&0&0&0&0.01&0&0&0&0.02&0&0&0&0&0&0&0&0&0&1.00&0&0&0&-0.01&0&0\\
0&0&0&0&0&0.00&0&0&0&0&0&0&0&0&0&0&0&0&0&1.02&0&0&0&0.00&0\\
-0.02&0&0&0&0&0&-0.02&0&0&0&0&0&0&0&0&0&-0.02&0&0&0&0.95&0&0&0&-0.02\\
0&0&0&0&0&0&0&0.00&0&0&0&0&0&0&0&0&0&0.00&0&0&0&1.02&0&0&0\\
0&0&0&0&0.02&0&0&0&0.01&0&0&0&0&0&0&0&0&0&-0.01&0&0&0&1.00&0&0\\
0&0&0&0&0&-0.00&0&0&0&0&0&0&0&0&0&0&0&0&0&0.00&0&0&0&1.01&0\\
-0.01&0&0&0&0&0&0.02&0&0&0&0&0&0&0&0&0&-0.03&0&0&0&-0.02&0&0&0&0.99
\end{bmatrix}
$$

$$[P_{N=941}]\big/C_3(941) \qquad C_3(941) = 552$$

$$[P_N]_{l',m';l,m} := \langle N; l', m' | N; l, m \rangle = 4\pi \sum_{|\mathbf{n}|^2=N} Y^*_{l'm'}(\hat{\mathbf{n}}) Y_{lm}(\hat{\mathbf{n}})$$

25×25 matrix ordered as $(l, m) = (0,0), (1,-1), (1,0), (1,1), \cdots, (4,4)$

Resonance

(Mass , Width, Pole position, Coupling)

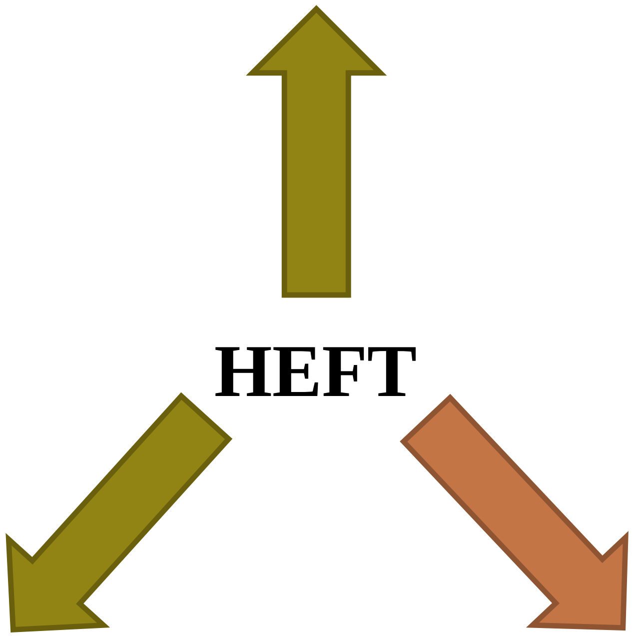

T matrix
(Phase Shifts, inelasticity)

Lattice Spectrum

Introduction of HEFT

Y. Li etc. PRD 101(2020), 114501
PRD 103(2021), 094518

- **Partial Wave Mixing**

$$|\mathbf{n}\rangle \xrightarrow{\sum_{\hat{\mathbf{n}}} Y_{lm}(\hat{\mathbf{n}})\,|\mathbf{n}\rangle} |N;l,m\rangle \xrightarrow{\sum_m [C_l]_{\Gamma,f,\alpha;m}\,|N;l,m\rangle} |N,l;\Gamma,f,\alpha\rangle \xrightarrow{\text{Orthonormalization}} |N;\Gamma,F,\alpha\rangle$$

$$[P_N]_{l',m';l,m} := \langle N;l',m'|N;l,m\rangle = \sum_{\hat{\mathbf{n}}} Y^*_{l'm'}(\hat{\mathbf{n}})Y_{lm}(\hat{\mathbf{n}})$$

25×25 for $l_{\text{cut}} = 4$ $\xrightarrow{[C]^\dagger[P][C]}$ 2×2 block $\mathbf{A}_1^+$

$$[P_{N;\Gamma,\alpha}]_{l',f';l,f} := \langle N,l';\Gamma,f',\alpha|N,l;\Gamma,f,\alpha\rangle = \sum_{m',m} [C_{l'}]^*_{\Gamma,f',\alpha;m'}[P_N]_{l',m';l,m}[C_l]_{\Gamma,f,\alpha;m}$$

Combination Coefficients: $[G_{l;\Gamma}]_{N',F';N,F} = \sum_f \langle N';\Gamma,F',\alpha|N';l,\Gamma,f,\alpha\rangle\,\langle N;l,\Gamma,f,\alpha|N;\Gamma,F,\alpha\rangle$

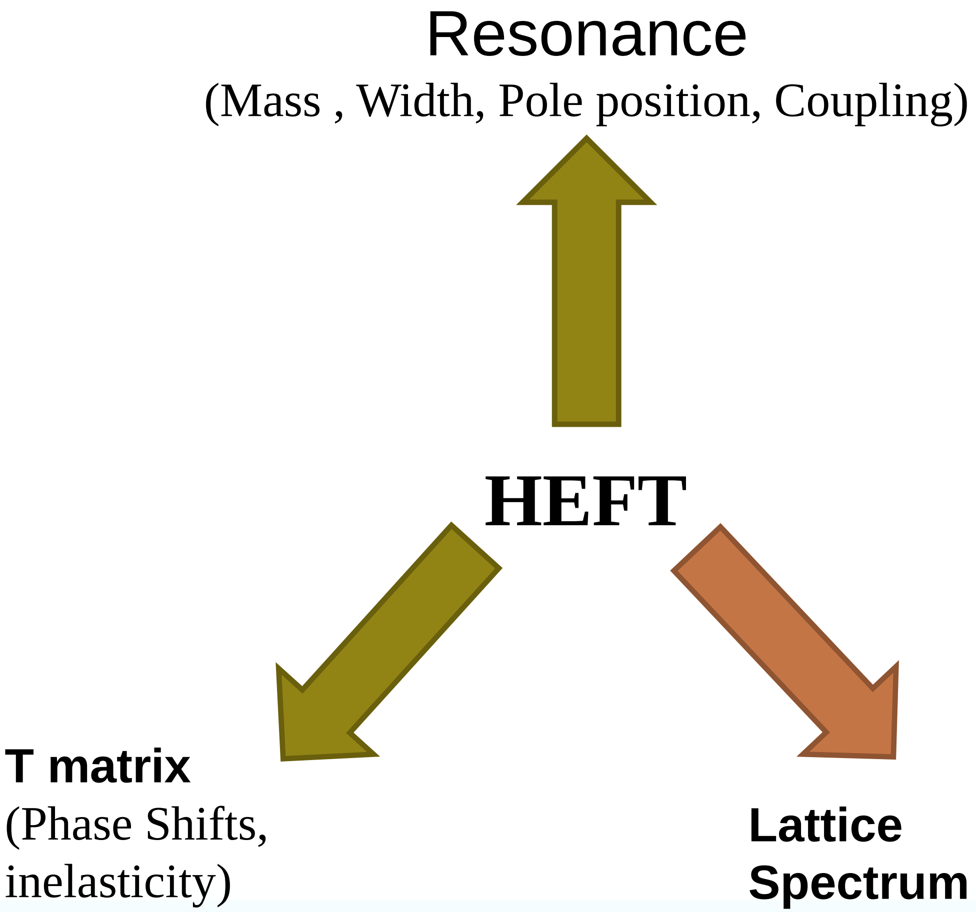

Introduction of HEFT

Y. Li etc. PRD 101(2020), 114501
PRD 103(2021), 094518

- **Analysis the ππ scattering with I=2**
  - $l_{\text{cut}} = 4$, only s-, d- and g-waves are present
  - Separable potential model:

$$v_l(p,k) = f_l(p) G_l f_l(k)$$

$$f_l(k) \sim \frac{(d_l \times k)^l}{(1 + (d_l \times k)^2)^{l/2+2}}$$

  - 6 parameters: $G_0, G_2, G_4, d_0, d_2, d_4$
  - Dimensions of Hamiltonians ($N_{\text{cut}} = 600$):

$$\mathbf{A}_1^+ : 923 \quad \mathbf{E}^+ : 965 \quad \mathbf{T}_2^+ : 963$$

  - The fitted data: 11 energy levels

PRD 86, 034031 (2012)
Jozef J. Dudek et al.

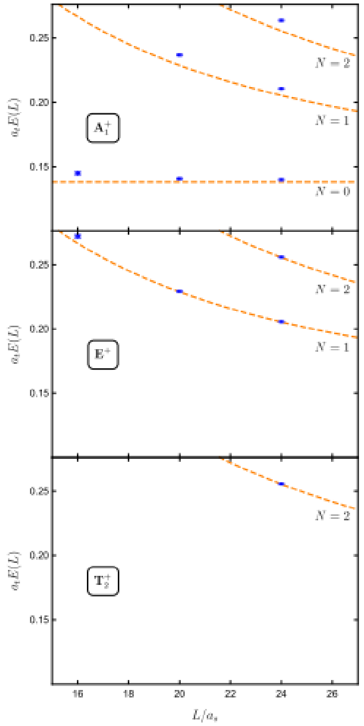

Resonance
(Mass , Width, Pole position, Coupling)

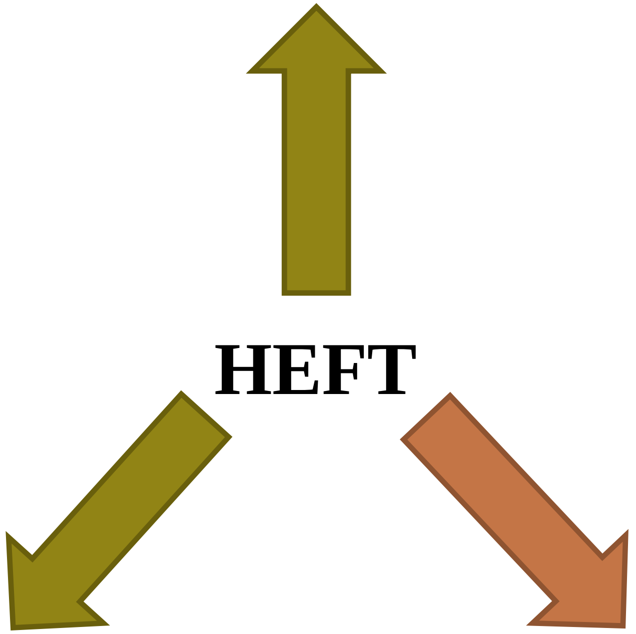

HEFT

T matrix
(Phase Shifts, inelasticity)

Lattice Spectrum

Introduction of HEFT

Y. Li etc. PRD 101(2020), 114501
PRD 103(2021), 094518

- **Analysis the ππ scattering with I=2**

Components of eigenstates

A_1^+	$N=0$	$N=1$	$N=2$	$N=3$	$N=4$	$\cdots$
1st	99.7	0.2	0.0	0.0	0.0	$\cdots$
2nd	0.1	97.4	1.9	0.2	0.0	$\cdots$
3rd	0.0	1.5	94.5	2.8	0.3	$\cdots$

Volume dependent spectra

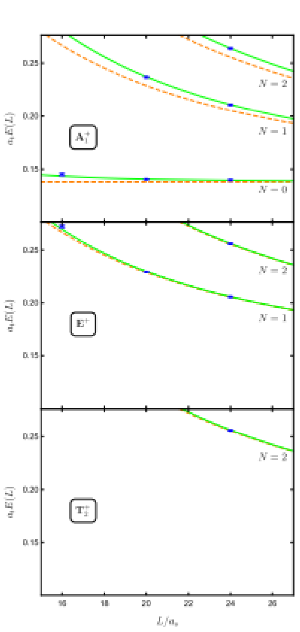

Phase shifts with errors

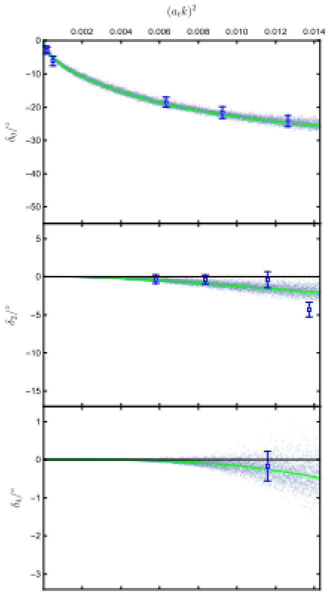

- Fitting $\to$ Parameters $\to$ $\hat{H}$ and $\hat{H}_L$
- $\hat{H} \to \delta_l(E)$
- $\hat{H}_L \to E_n(\Gamma, L)$
- $\hat{H}_L \to$ Eigenstates

Resonance
(Mass , Width, Pole position, Coupling)

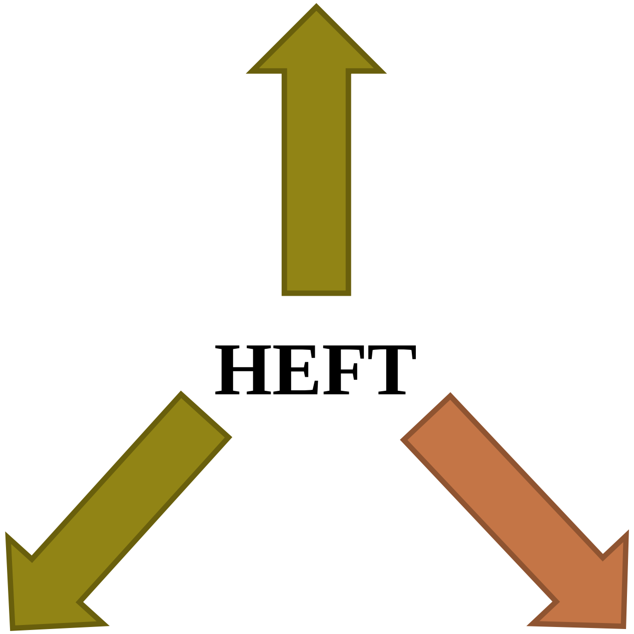

HEFT

T matrix
(Phase Shifts, inelasticity)

Lattice Spectrum

Introduction of HEFT

Y. Li etc. PRD 101(2020), 114501
PRD 103(2021), 094518

- **Partial Wave Mixing, Moving system, Elongated volume**

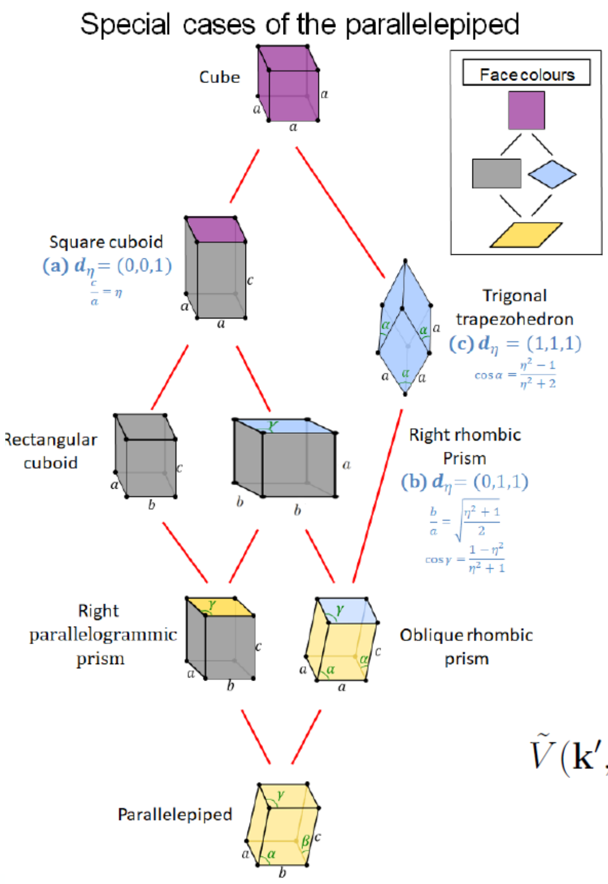

	Moving	Elongated	mass
A:	No	No	any
B:	Yes	Yes	unequal
C1:	No	Yes	any
C2:	Yes	Yes	equal

Case	A	B	C1 or C2
G_∞	O(3)	O(2)	$\mathrm{O}(2)\times \mathrm{C}_2$
$(\Gamma_\infty, \alpha_\infty)$	$(l^{\mathcal{P}}, m)$	$(\lvert m\rvert, S_m)$	$(\lvert m\rvert^{\mathcal{P}}, S_m)$
$\tilde{v}_{\Gamma_\infty}$	v_l	$\mathcal{J}^{\frac{1}{2}}(\mathbf{k}')\,\mathcal{J}^{\frac{1}{2}}(\mathbf{k})\sum_l v_l \frac{2l+1}{4\pi}\frac{(l-m)!}{(l+m)!} \times P_{lm}(\cos\theta'^*)P_{lm}(\cos\theta^*)$	$\mathcal{J}^{\frac{1}{2}}(\mathbf{k}')\,\mathcal{J}^{\frac{1}{2}}(\mathbf{k})\sum_{l^{\mathcal{P}}} v_l \frac{2l+1}{4\pi}\frac{(l-m)!}{(l+m)!} \times P_{lm}(\lvert\cos\theta'^*\rvert)P_{lm}(\lvert\cos\theta^*\rvert)$
$u_{\Gamma_\infty,\alpha_\infty}$	Y_{lm}	$e^{im\phi^*}$	$S^{\mathcal{P}}(m,\theta^*)\,e^{im\phi^*}$

$$\tilde{V}(\mathbf{k}', \mathbf{k}) = \sum_{\Gamma_\infty} \tilde{v}_{\Gamma_\infty}(e'_n, e_n) \sum_{\alpha_\infty} u_{\Gamma_\infty,\alpha_\infty}(\mathbf{n}')\, u^*_{\Gamma_\infty,\alpha_\infty}(\mathbf{n})$$

Resonance
(Mass , Width, Pole position, Coupling)

HEFT

T matrix
(Phase Shifts, inelasticity)

Lattice Spectrum

Introduction of HEFT

Y. Li etc. PRD 101(2020), 114501
PRD 103(2021), 094518

- **Analysis the ππ scattering with I=2**

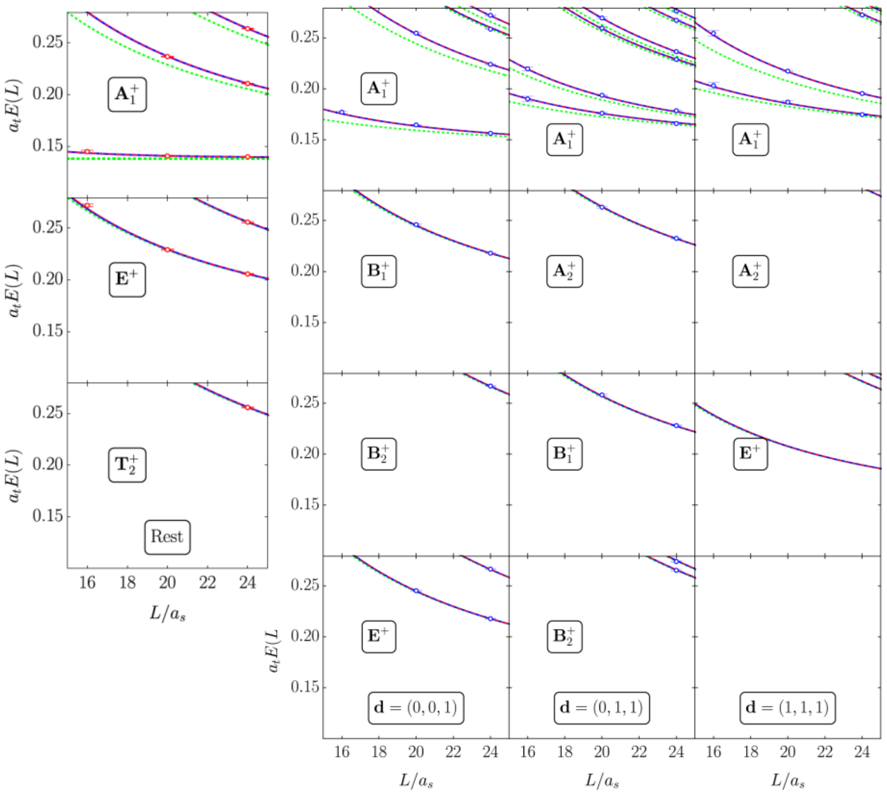

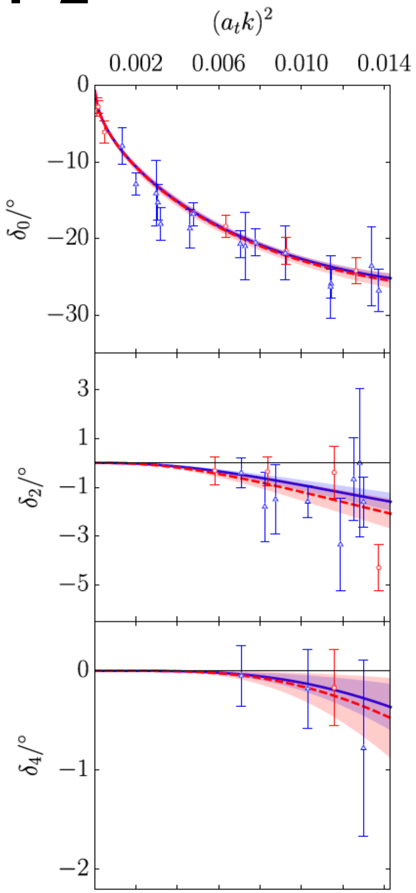

Resonance
(Mass , Width, Pole position, Coupling)

HEFT

T matrix
(Phase Shifts, inelasticity)

Lattice Spectrum

Introduction of HEFT

Y. Li etc. PRD 101(2020), 114501
PRD 103(2021), 094518

- **Analysis the ππ scattering with I=2**

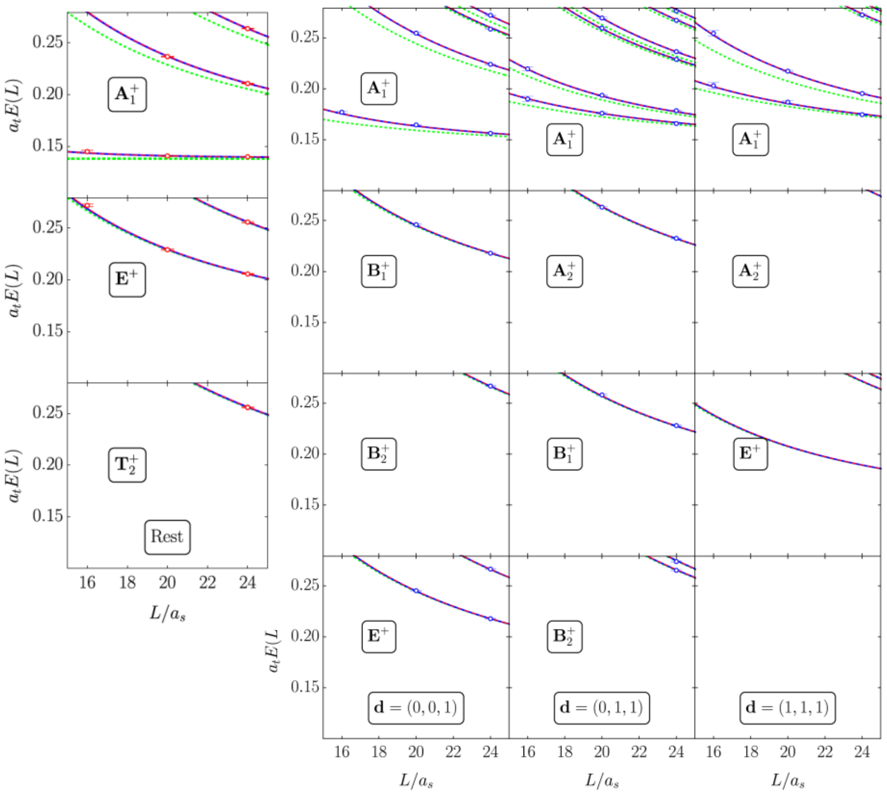

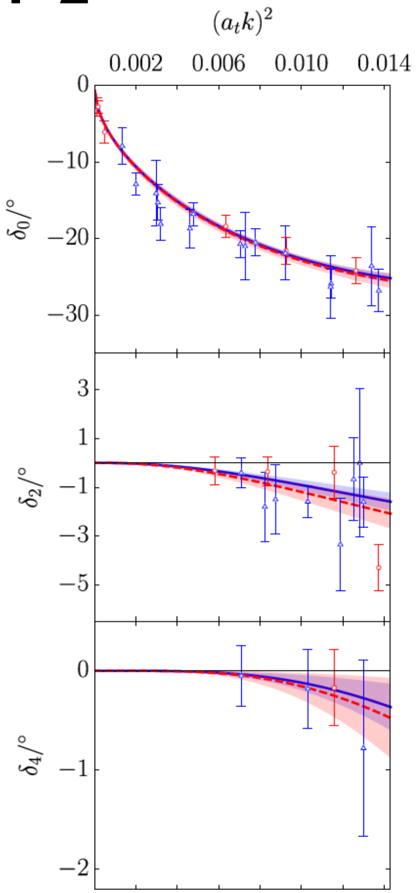

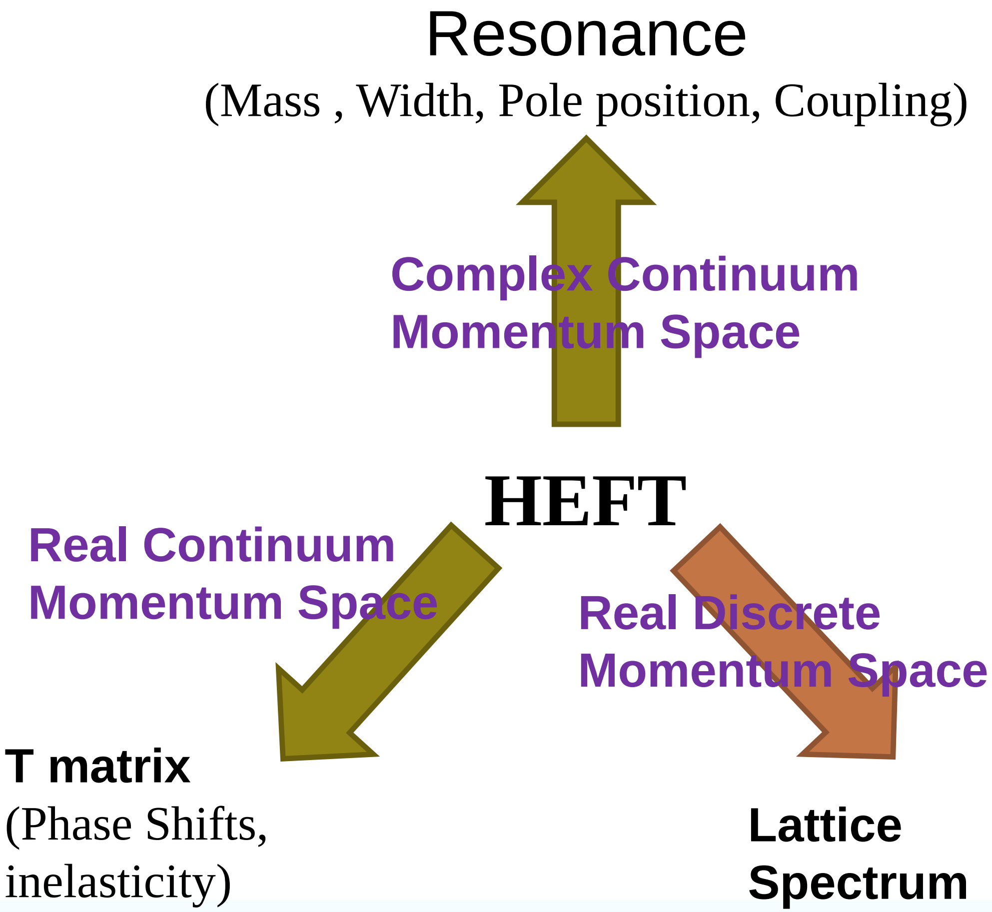

Introduction of HEFT

HEFT:

1. Build a Hamiltonian model;

2. If Experimental data available, we fit Experimental data to fix the parameters in the model;
   If Lattice data available (close to physical pion mass), we fit these data;
   If both, we can use both of them constraint the model parameters.
   If we only have Lattice data with unphysical pion mass, we need another parameter for the mass dependence, such as mass slope.

3. From the fixed Hamiltonian, we can study the properties of Resonance. Especially, from the eigenvector in the finite volume, we can estimate the internal structure of the hadron.

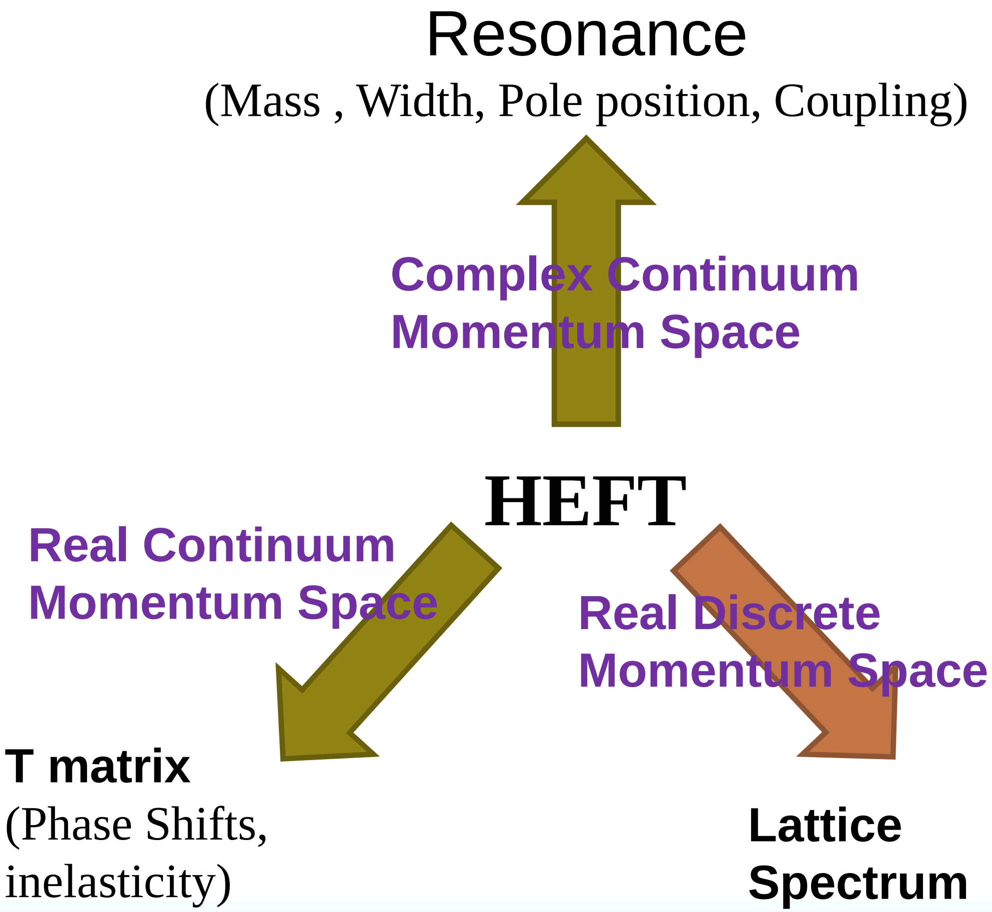

$\Lambda^*(1405)$

Zhan-wei Liu etc. Phys.Rev. D95 (2017) no.1, 014506

- I=0, $\pi\Sigma$, $\bar{K}N$, $\eta\Lambda$ and $\bar{K}\Xi$
- I=1, $\pi\Sigma$, $\bar{K}N$, $\pi\Lambda$

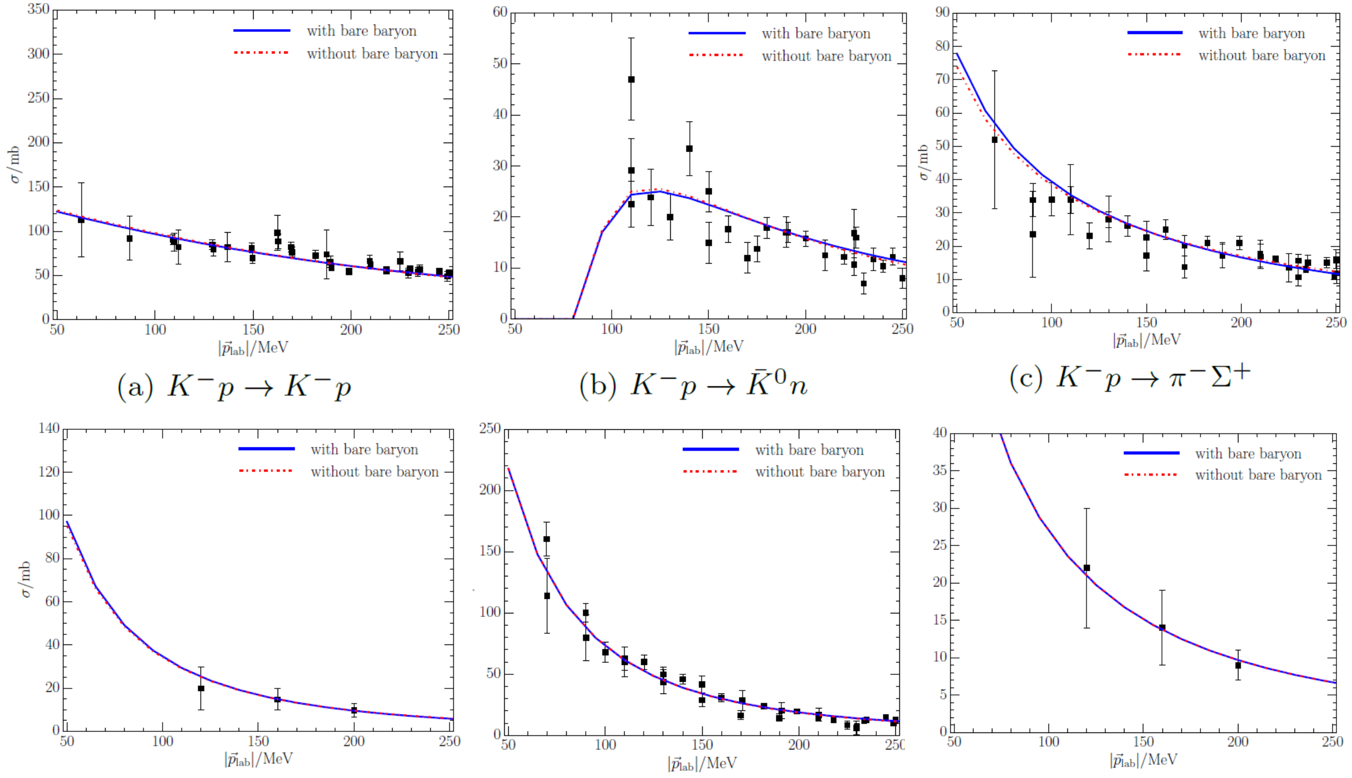

(a) $K^-p \to K^-p$ (b) $K^-p \to \bar{K}^0 n$ (c) $K^-p \to \pi^-\Sigma^+$

(d) $K^-p \to \pi^0\Sigma^0$ (e) $K^-p \to \pi^+\Sigma^-$ (f) $K^-p \to \pi^0\Lambda$

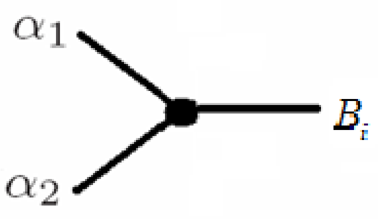

$$\frac{\sqrt{3}g^I_{\alpha,B_0}}{2\pi f}\sqrt{\omega_\pi(k)}u(k)$$

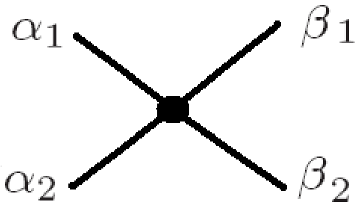

$$g^I_{\alpha,\beta}\frac{[\omega_{\alpha_M}(k)+\omega_{\beta_M}(k')]\,u(k)u(k')}{8\pi^2 f^2\sqrt{2\omega_{\alpha_M}(k)}\sqrt{2\omega_{\beta_M}(k')}}$$

Weinberg – Tomozawa Term

Λ*(1405)

Zhan-wei Liu etc. Phys.Rev. D95 (2017) no.1, 014506

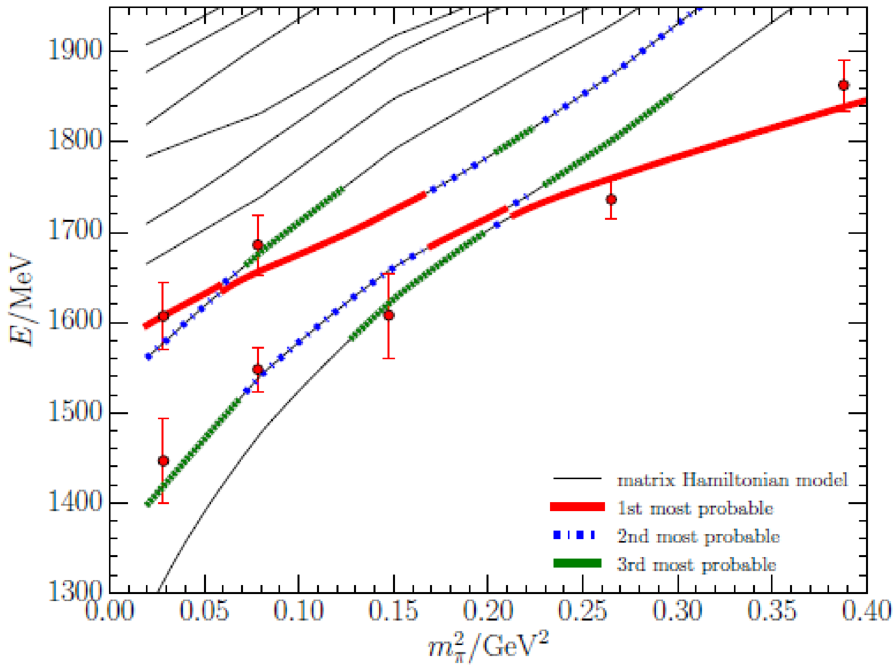

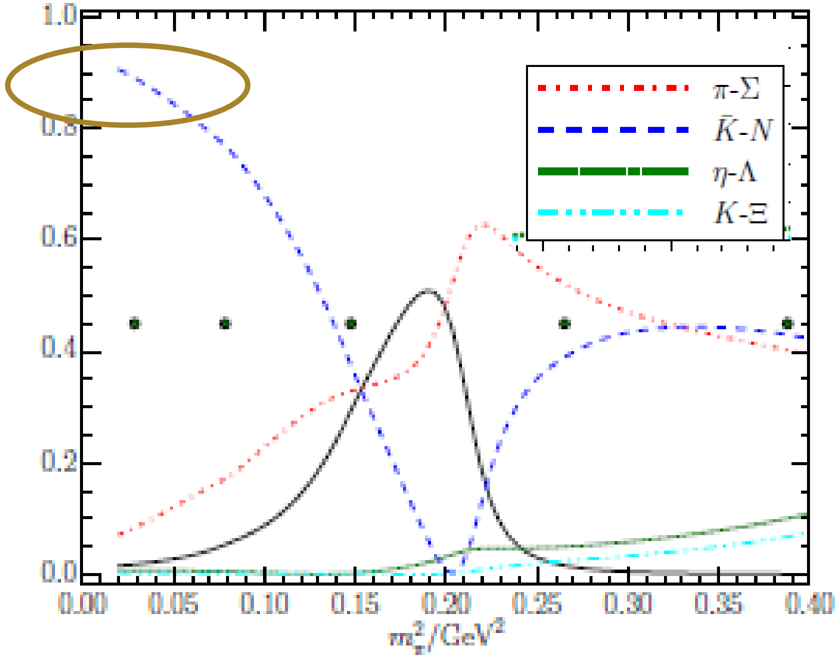

the Λ*(1405) is predominantly a molecular $\bar{\mathrm{K}}$ N bound State,

N*(1535)

Zhan-wei Liu etc. Phys.Rev.Lett. 116 (2016) no.8, 082004

2 Channels: πN and ηN

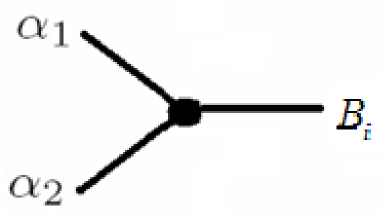

$$G^2_{iN}(k) = \left(3g^2_{N_0^* iN}/4\pi^2 f^2\right)\omega_i(k)u^2(k)$$

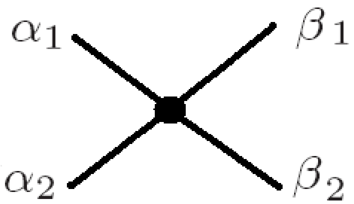

$$\frac{3g^S_{\pi N}\tilde{u}(k)\tilde{u}(k')}{4\pi^2 f^2}$$

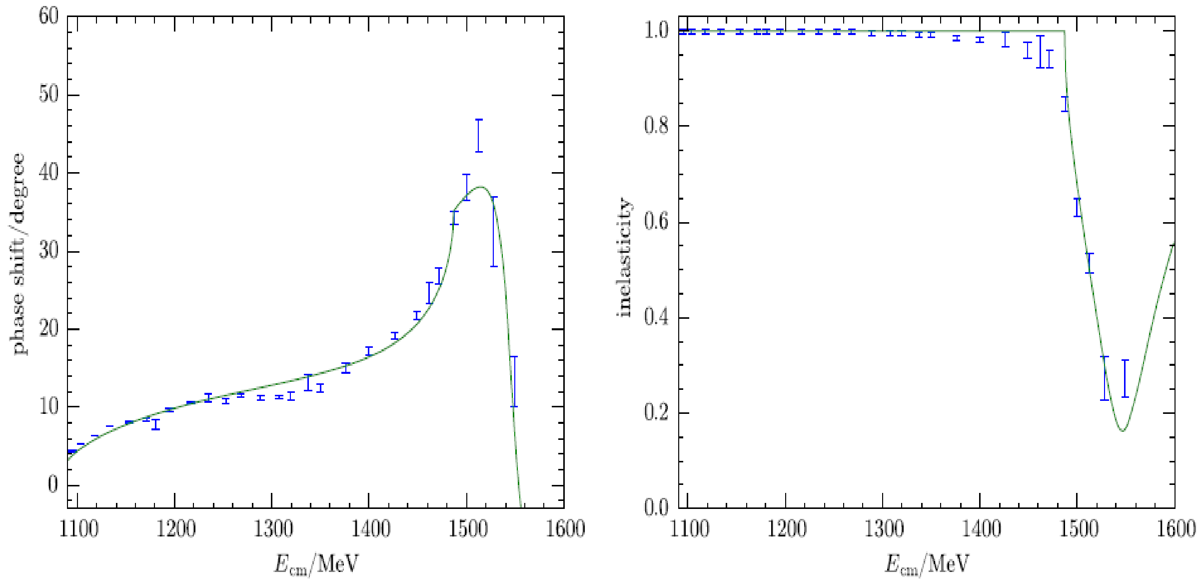

$$g^S_{\pi N} = -0.0608 \pm 0.0004$$
$$m_0 = 1601 \pm 14 \text{ MeV}$$
$$g_{N_0^*\pi N} = 0.186 \pm 0.006$$
$$g_{N_0^*\eta N} = 0.185 \pm 0.017$$

$$\chi^2_{\mathrm{DOF}} = 6.8$$

$$1531 \pm 29 - i88 \pm 2 \text{ MeV}$$

N*(1535)

Zhan-wei Liu etc. Phys.Rev.Lett. 116 (2016) no.8, 082004

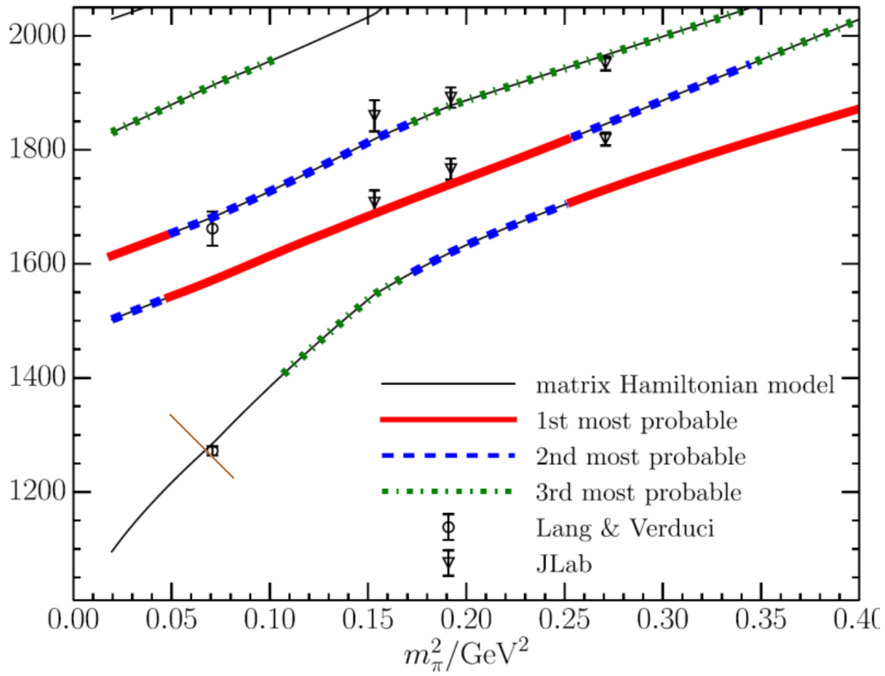

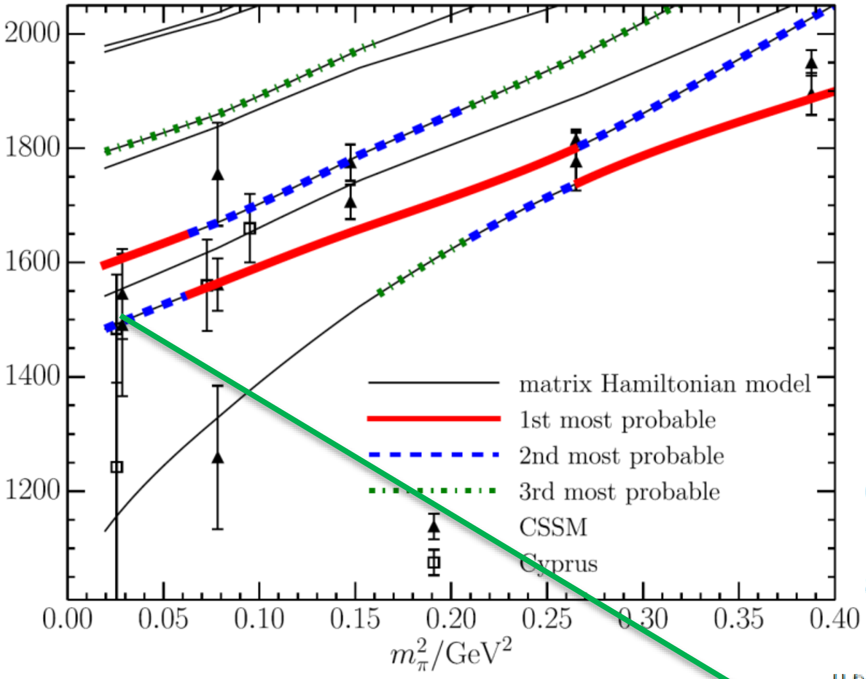

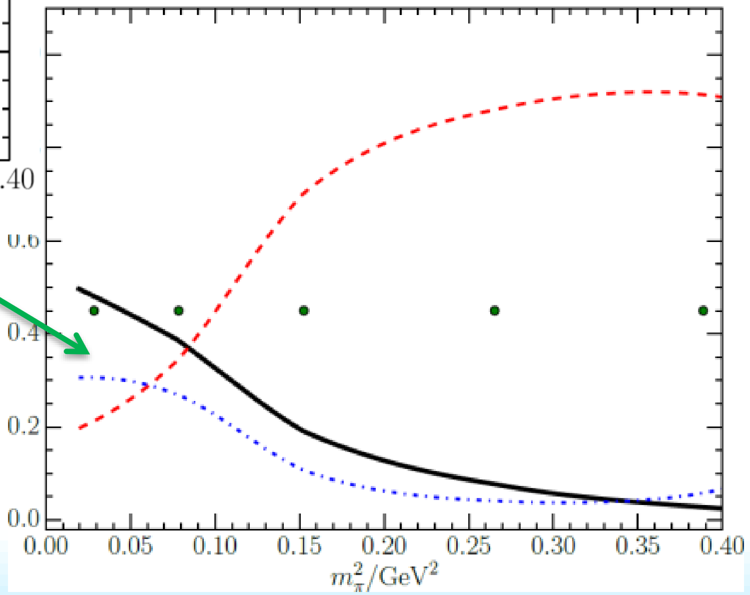

The main components (at least 50%) of N*(1535) is from the 3 quark core.

N*(1440)

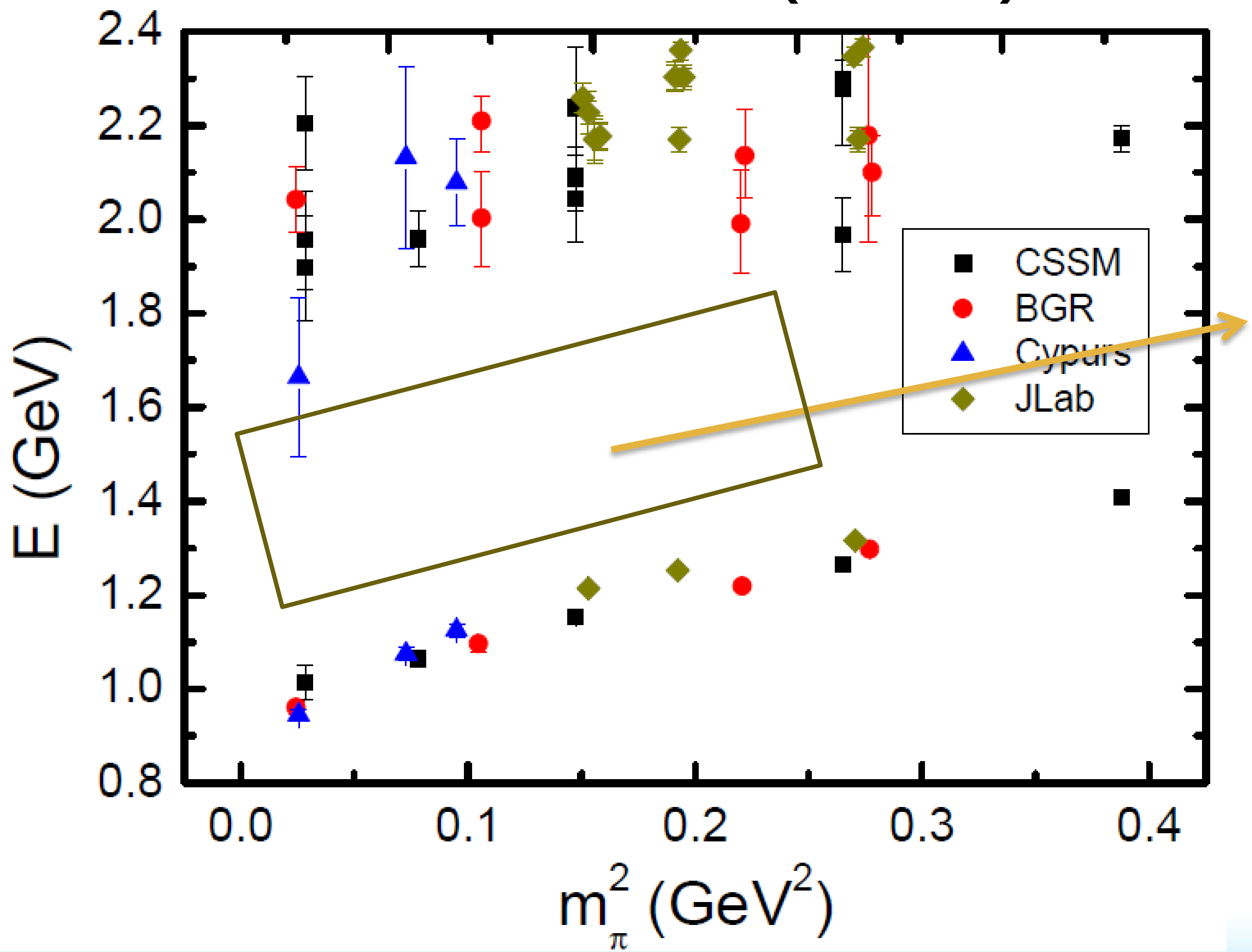

No State extracted from 3 quark operator

N*(1440)

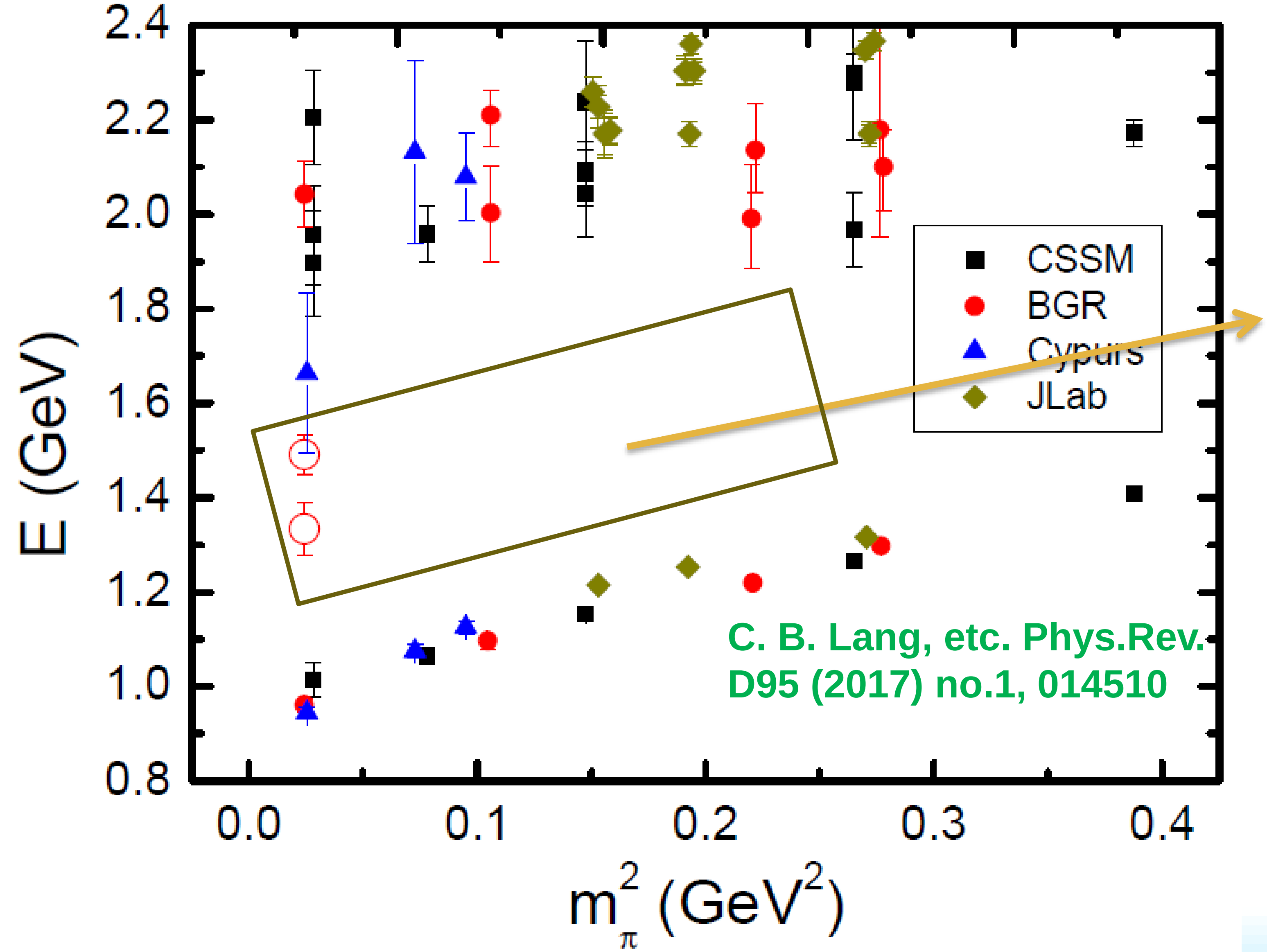

No State extracted from 3 quark operator

N*(1440)

Jia-jun Wu etc. arXiv: 1703.10715

Include 3 channels: πN, πΔ and σN

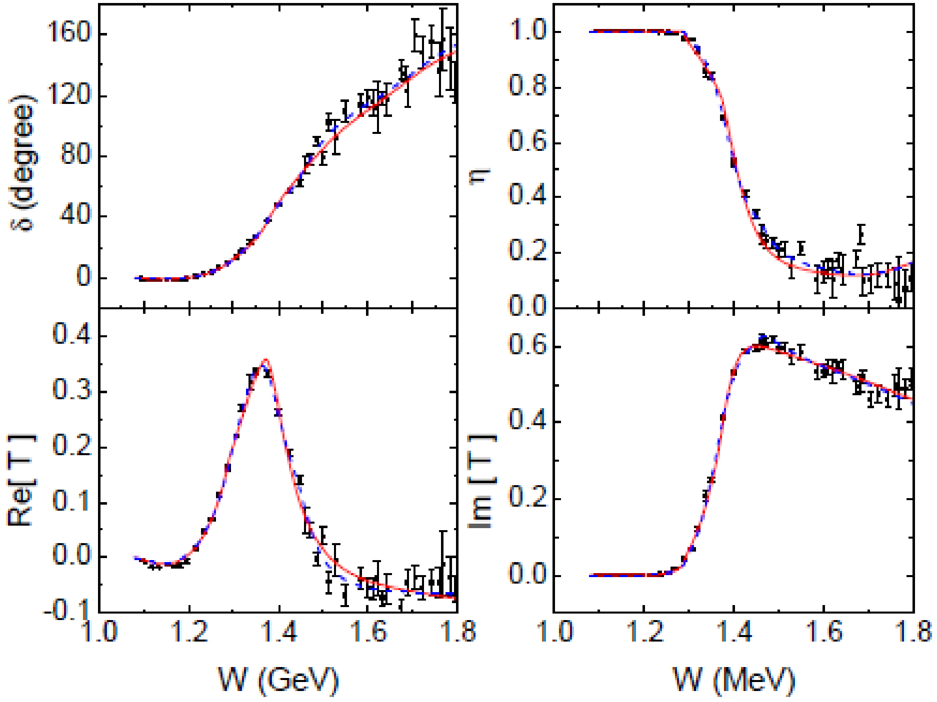

Parameter	I	II
$g^S_{\pi N,\pi N}$	1.156	0.634
$g^S_{\pi N,\pi\Delta}$	−0.662	−0.378
$g^S_{\pi N,\sigma N}$	−0.415	−1.738
$g^S_{\pi\Delta,\pi\Delta}$	−0.438	−0.581
$g^S_{\pi\Delta,\sigma N}$	1.332	0.964
$g^S_{\sigma N,\sigma N}$	10.000	10.000
m^0_B/GeV	2.000	1.7000
$g_{B_0\pi N}$	0.268	0.954
$g_{B_0\pi\Delta}$	1.544	−0.118
$g_{B_0\sigma N}$	−	−2.892
$\Lambda_{\pi N}$/GeV	0.5953	0.6302
$\Lambda_{\pi\Delta}$/GeV	1.5000	1.4318
$\Lambda_{\sigma N}$/GeV	1.5000	1.4533
Pole (MeV) (uuu)	$2012.28 - 42.09\,i$	$1355.57 - 70.81\,i$
Pole (MeV) (upu)	$1392.92 - 167.13\,i$	$1362.33 - 100.53\,i$

Bare state dominate

Meson-Baryon channel interaction dominate

Experimental data can not distinguish these two models

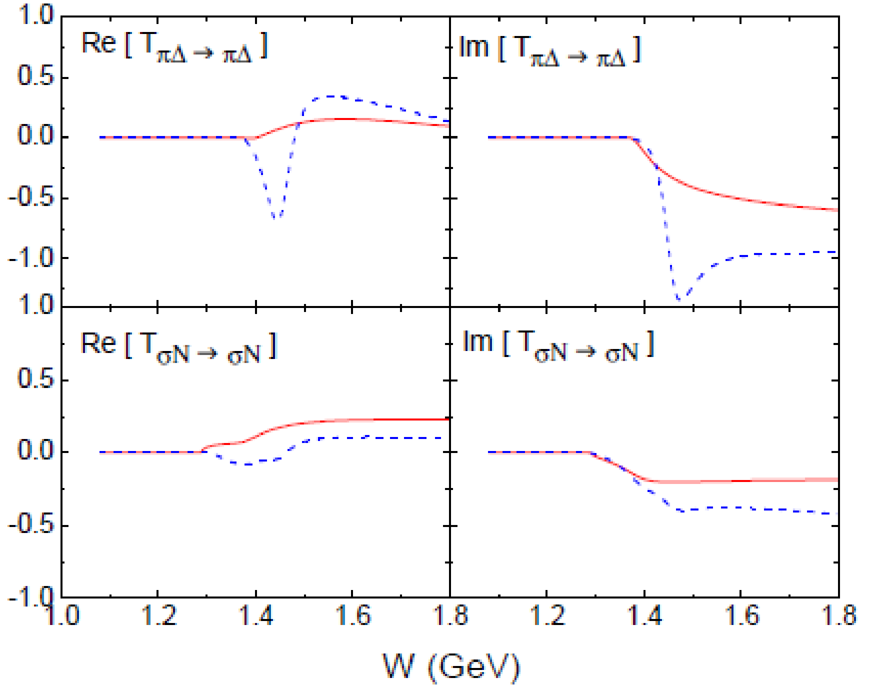

N*(1440)

Jia-jun Wu etc PRD97(2018) 094509

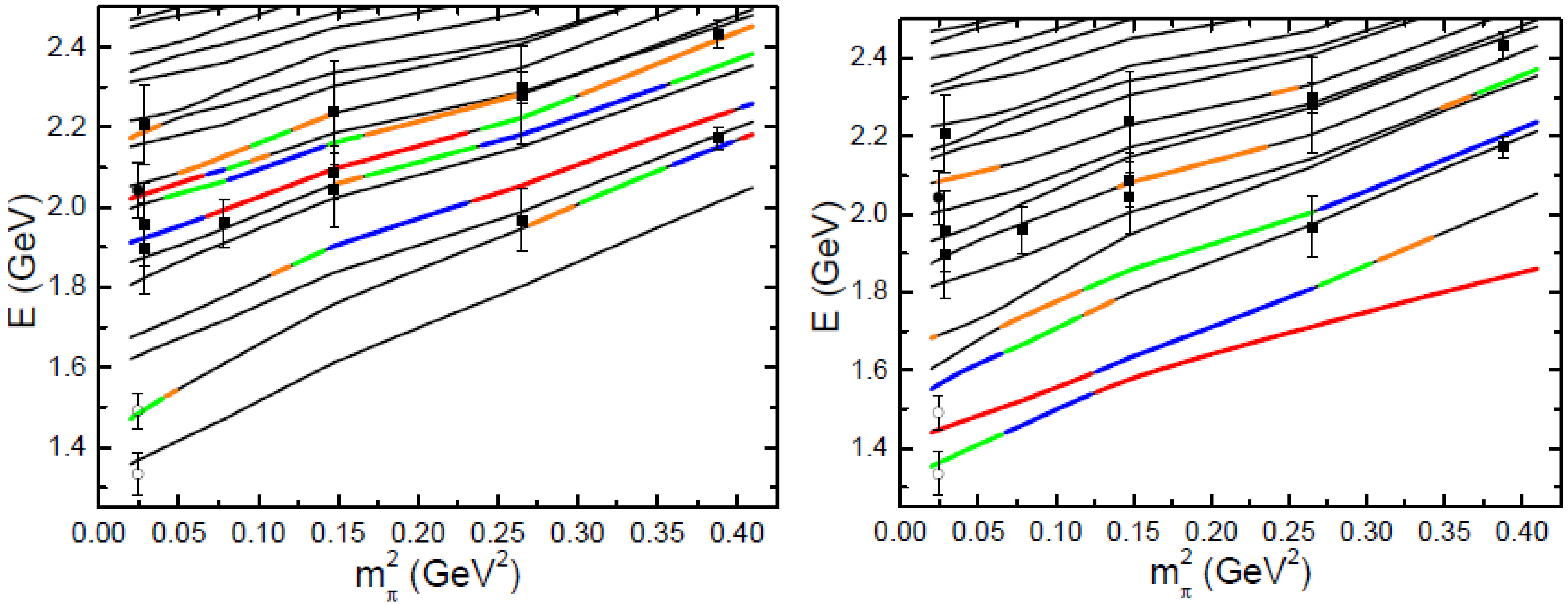

The first scenario with a bare state for P11 around the pole at 2.0 GeV can fit both Lattice data and experimental data well, it indicates that N*(1440) seems a re-scattering state, and first radial excitation of nucleon should be around 2.0 GeV.

N*(1440)

Jia-jun Wu etc PRD97(2018) 094509

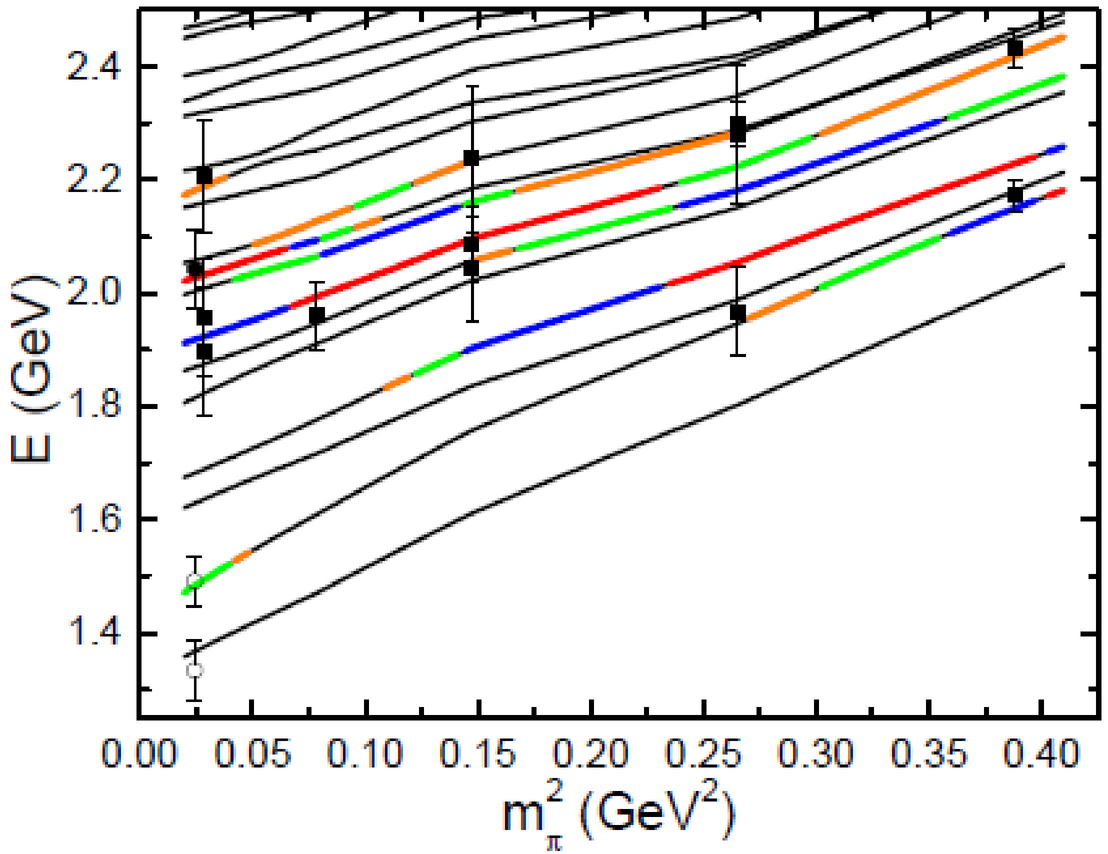

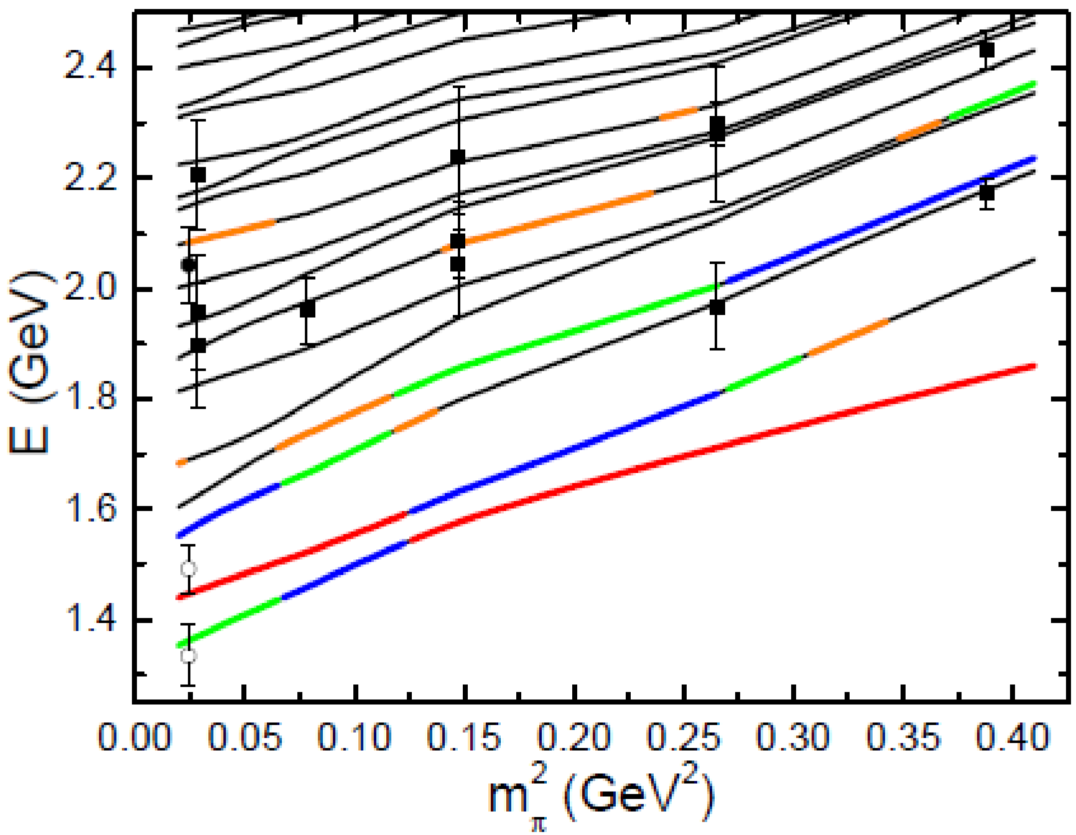

The first scenario with a bare state for P11 around the pole at 2.0 GeV can fit both Lattice data and experimental data well, it indicates that N*(1440) seems a re-scattering state, and first radial excitation of nucleon should be around 2.0 GeV.

The Second scenario with a bare state for N*(1440) fit the experimental data well. But the largest possibility for bare state does not touch the lattice point. Thus, it fails to explain Lattice data.

N*(1440)

Jia-jun Wu etc PRD97(2018) 094509

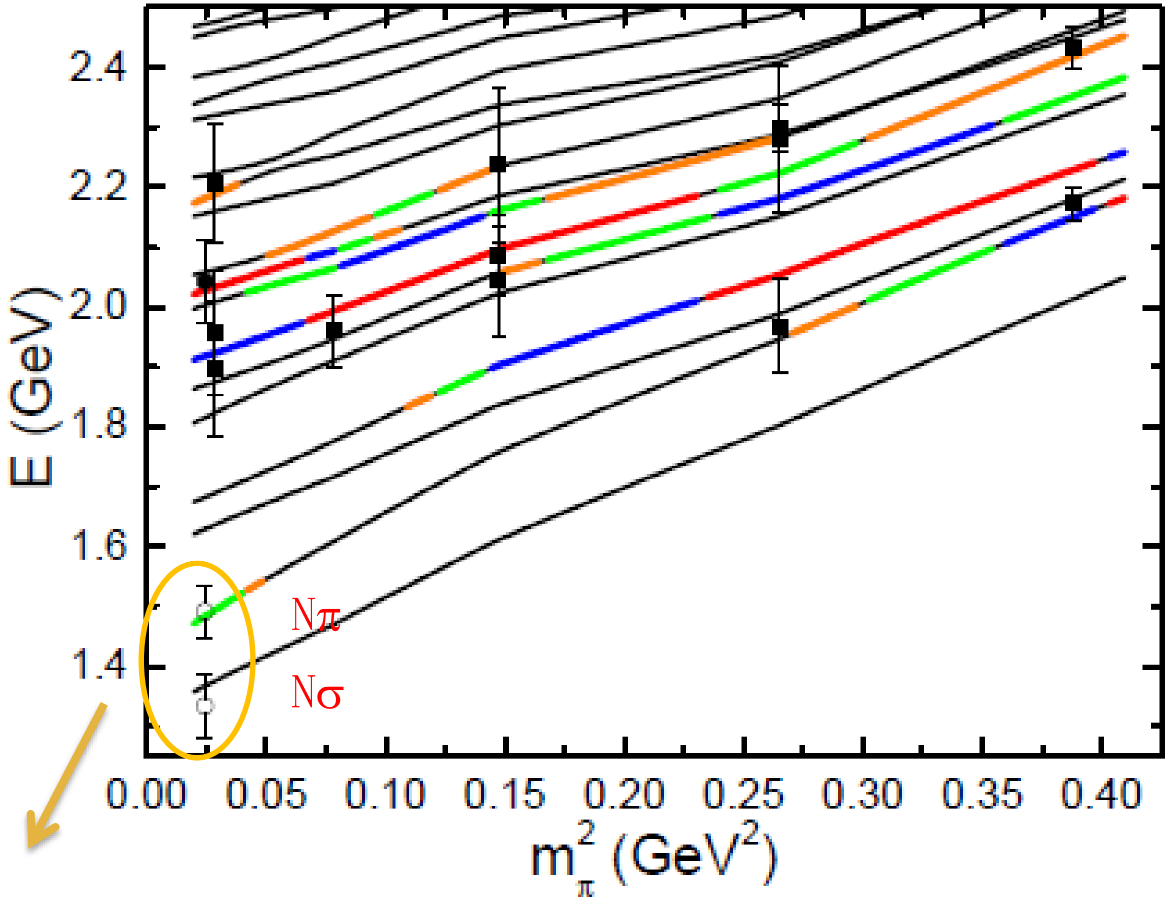

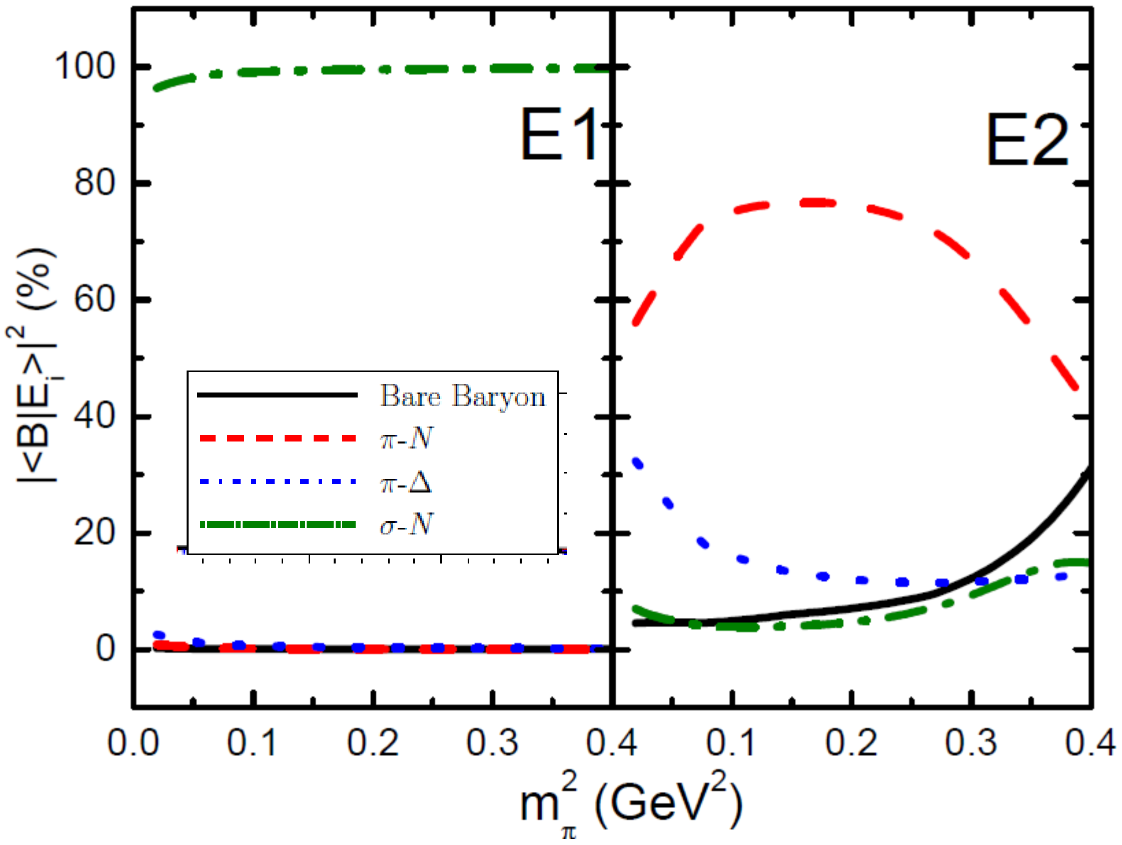

It is not a FIT !!!

C. B. Lang, etc. Phys.Rev. D95 (2017) no.1, 014510

We need more data and detailed study, for the contribution from $N\pi\pi$ three body.

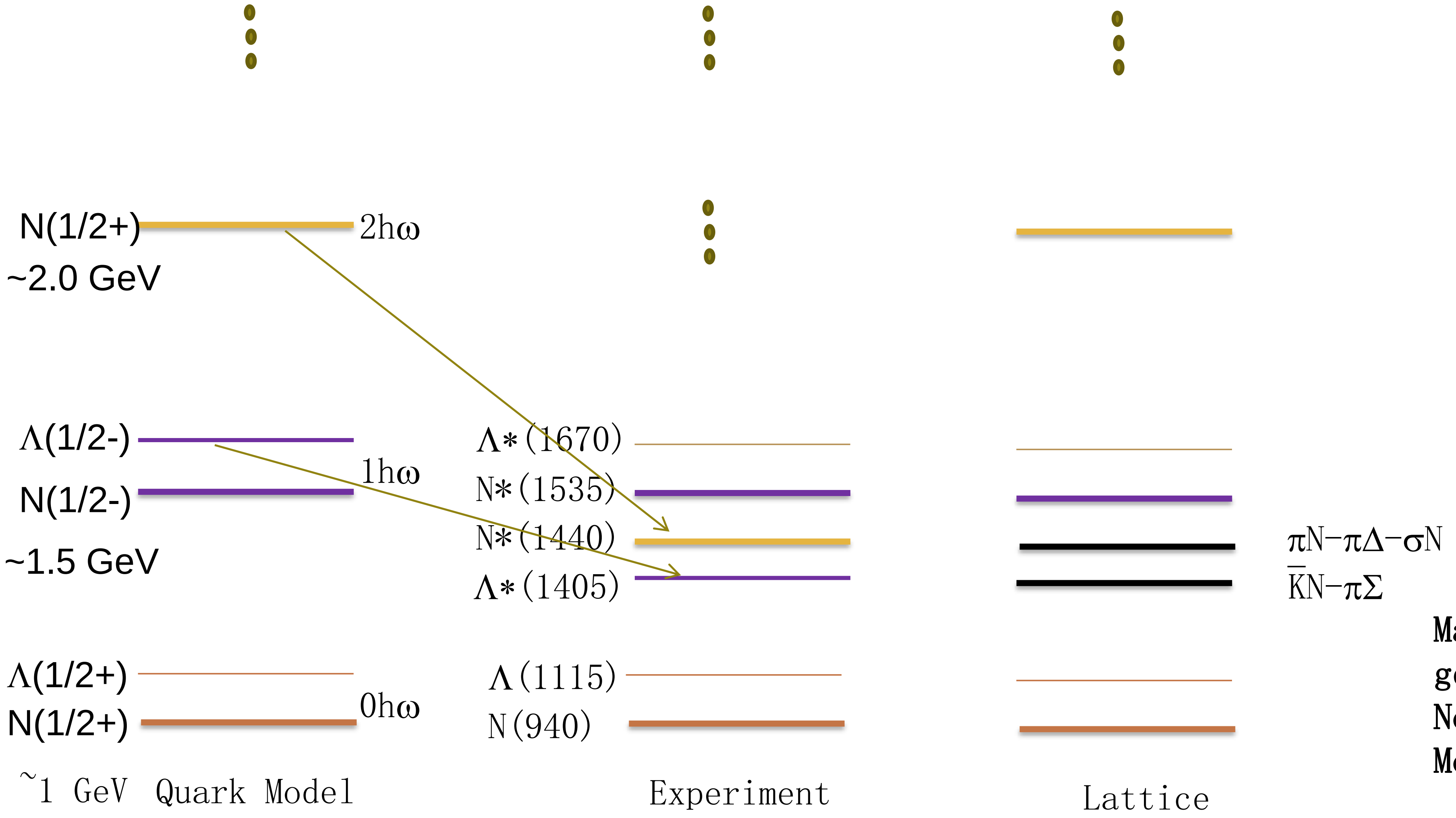

Mainly Dynamical generated states. Not in the Quark Model

$D_{s0}(2317)$, $D_{s1}(2460)$, $D_{s1}(2536)$, $D_{s2}(2573)$

Z. Yang, G.-J. Wang, J.-j. Wu, S.-l. Zhu, M. Oka **Phys.Rev.Lett.128(2020),112001**

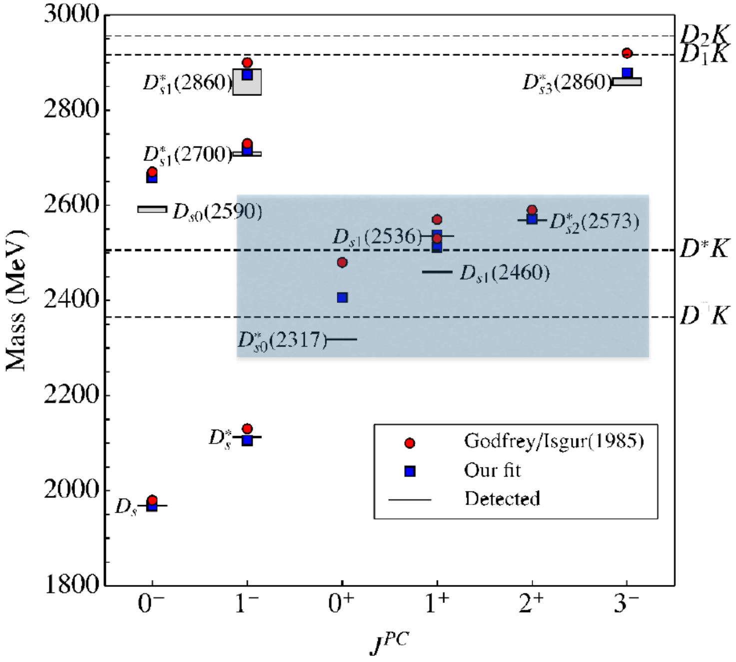

$D_{s0}(2317)$, $D_{s1}(2460)$, $D_{s1}(2536)$, $D_{s2}(2573)$

Z. Yang, G.-J. Wang, J.-j. Wu, S.-l. Zhu, M. Oka **Phys.Rev.Lett.128(2020),112001**

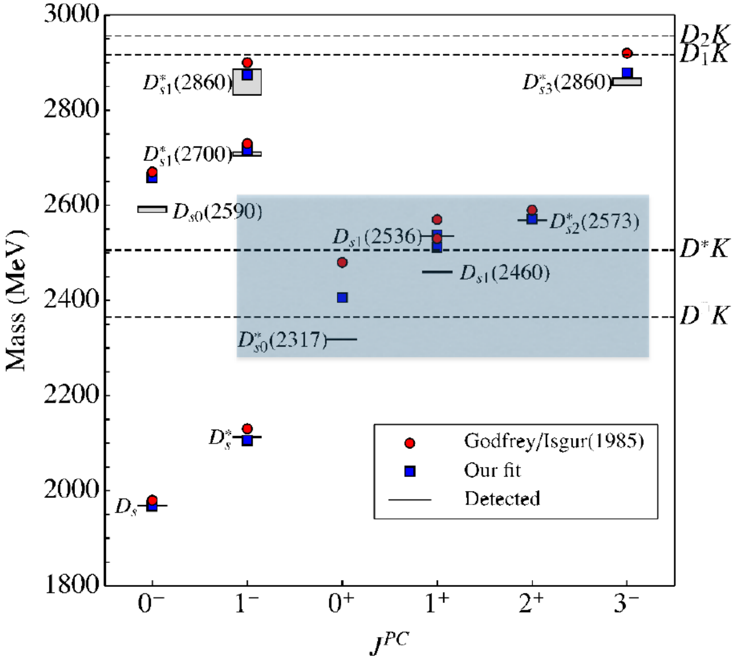

	$\bar{c}s$ cores		channel	
	$B(\|^{2S+1}L_J\rangle)$	B(mass)	α	L
$D_{s0}^*(2317)$	$\|^3P_0\rangle$	2405.9	DK	S
$D_{s1}^*(2460)$	$0.68\|^1P_1\rangle - 0.74\|^3P_1\rangle = -0.99\phi_s + 0.13\phi_d$	2511.5	D^*K	S, D
$D_{s1}^*(2536)$	$-0.74\|^1P_1\rangle - 0.68\|^3P_1\rangle = -0.13\phi_s - 0.99\phi_d$	2537.8	D^*K	S, D
$D_{s2}^*(2573)$	$\|^3P_2\rangle$	2571.2	DK, D^*K	D

1. Fix the bare mass and wave function from GI model；

$D_{s0}(2317)$, $D_{s1}(2460)$, $D_{s1}(2536)$, $D_{s2}(2573)$

Z. Yang, G.-J. Wang, J.-j. Wu, S.-l. Zhu, M. Oka **Phys.Rev.Lett.128(2020),112001**

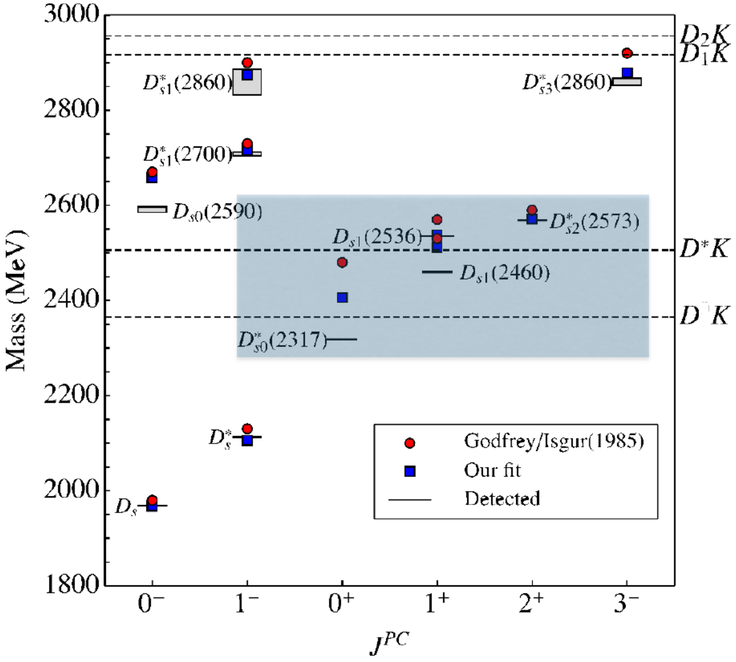

1. Fix the bare mass and wave function from GI model;
2. The interaction of bare-channel and channel-channel;

$^3P_0$ model

at quark level

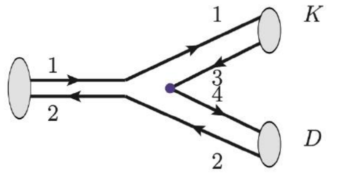

Figure 2: The diagram contribute to the process $D^*_s(2317) \to DK$.

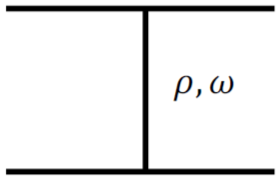

	$\bar{c}s$ cores		channel	
	$B(\|^{2S+1}L_J\rangle)$	B(mass)	α	L
$D^*_{s0}(2317)$	$\|^3P_0\rangle$	2405.9	DK	S
$D^*_{s1}(2460)$	$0.68\|^1P_1\rangle - 0.74\|^3P_1\rangle$ $= -0.99\phi_s + 0.13\phi_d$	2511.5	D^*K	S, D
$D^*_{s1}(2536)$	$-0.74\|^1P_1\rangle - 0.68\|^3P_1\rangle$ $= -0.13\phi_s - 0.99\phi_d$	2537.8	D^*K	S, D
$D^*_{s2}(2573)$	$\|^3P_2\rangle$	2571.2	DK, D^*K	D

$D_{s0}(2317)$, $D_{s1}(2460)$, $D_{s1}(2536)$, $D_{s2}(2573)$

Z. Yang, G.-J. Wang, J.-j. Wu, S.-l. Zhu, M. Oka **Phys.Rev.Lett.128(2020),112001**

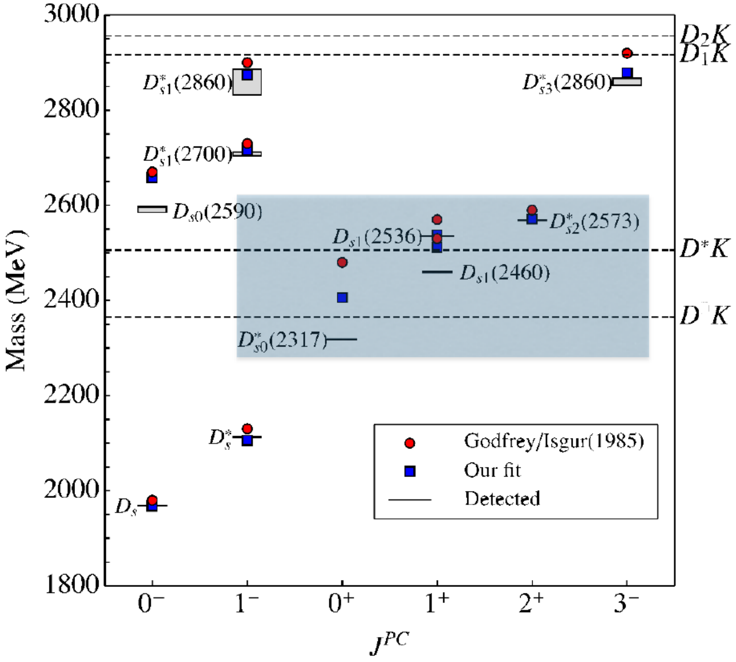

	$\bar{c}s$ cores		channel	
	$B(\vert^{2S+1}L_J\rangle)$	B(mass)	α	L
$D_{s0}^*(2317)$	$\vert^3P_0\rangle$	2405.9	DK	S
$D_{s1}^*(2460)$	$0.68\vert^1P_1\rangle - 0.74\vert^3P_1\rangle$ $= -0.99\phi_s + 0.13\phi_d$	2511.5	D^*K	S, D
$D_{s1}^*(2536)$	$-0.74\vert^1P_1\rangle - 0.68\vert^3P_1\rangle$ $= -0.13\phi_s - 0.99\phi_d$	2537.8	D^*K	S, D
$D_{s2}^*(2573)$	$\vert^3P_2\rangle$	2571.2	DK, D^*K	D

1. Fix the bare mass and wave function from GI model;
2. The interaction of bare-channel and channel-channel;

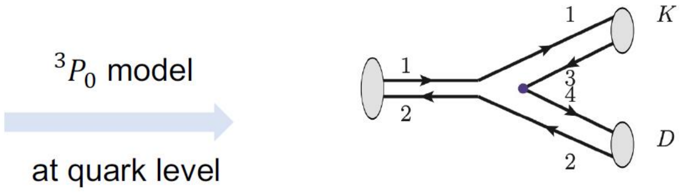

Figure 2: The diagram contribute to the process $D_s^*(2317) \to DK$.

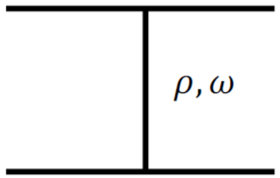

3. Fit Lattice data;

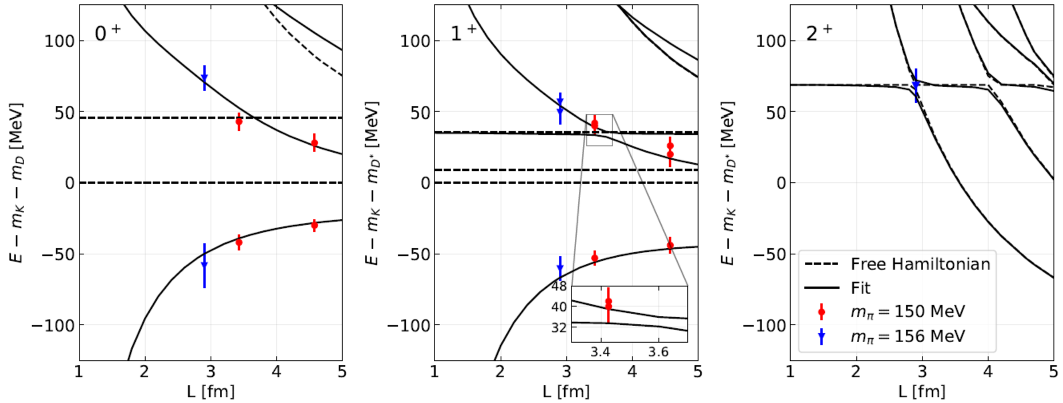

$D_{s0}(2317)$, $D_{s1}(2460)$, $D_{s1}(2536)$, $D_{s2}(2573)$

Z. Yang, G.-J. Wang, J.-j. Wu, S.-l. Zhu, M. Oka **Phys.Rev.Lett.128(2020),112001**

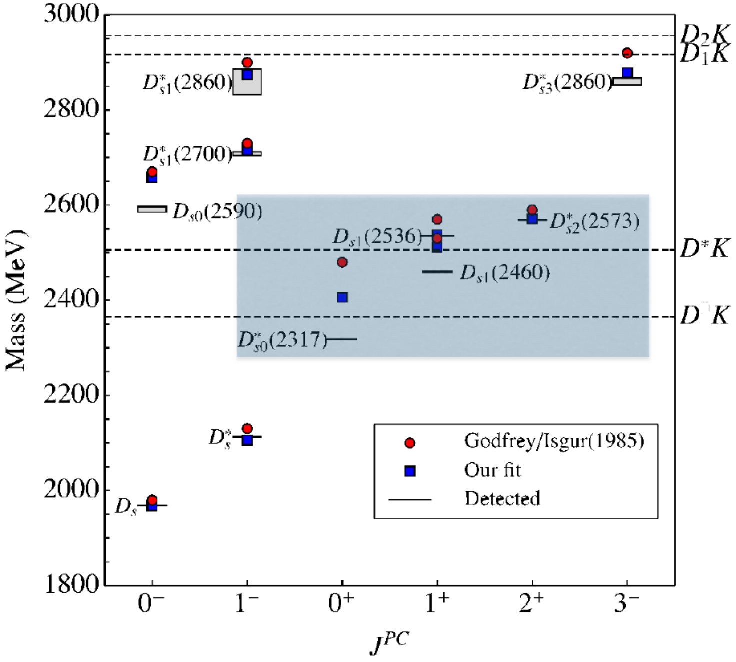

	$\bar{c}s$ cores		channel	
	$B(\|^{2S+1}L_J\rangle)$	B(mass)	α	L
$D^*_{s0}(2317)$	$\|^3P_0\rangle$	2405.9	DK	S
$D^*_{s1}(2460)$	$0.68\|^1P_1\rangle - 0.74\|^3P_1\rangle = -0.99\phi_s + 0.13\phi_d$	2511.5	D^*K	S, D
$D^*_{s1}(2536)$	$-0.74\|^1P_1\rangle - 0.68\|^3P_1\rangle = -0.13\phi_s - 0.99\phi_d$	2537.8	D^*K	S, D
$D^*_{s2}(2573)$	$\|^3P_2\rangle$	2571.2	DK, D^*K	D

1. Fix the bare mass and wave function from GI model;
2. The interaction of bare-channel and channel-channel;

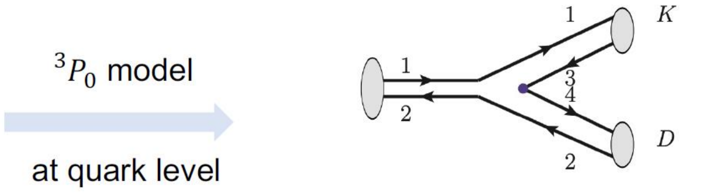

Figure 2: The diagram contribute to the process $D^*_s(2317) \to DK$.

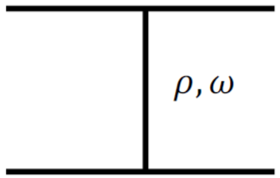

	$P(c\bar{s})$
$D^*_{s0}(2317)$	$\approx 32.0\%$
$D^*_{s1}(2460)$	$\approx 52.4\%$
$D^*_{s1}(2536)$	$\approx 98.2\%$
$D^*_{s2}(2573)$	$\approx 95.9\%$

3. Fit Lattice data;

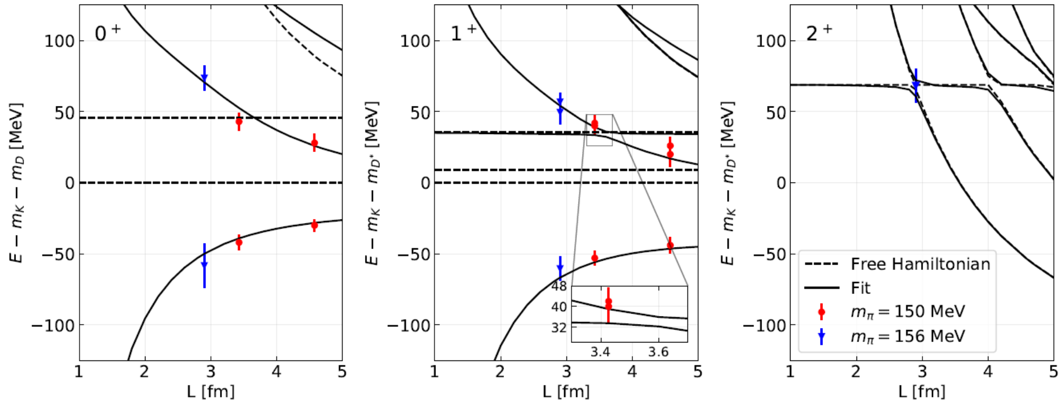

Conclusion:

$D^*_{s0}(2317)$-DK
$D_{s1}(2460)$-D*K
S-wave

Mass moving vs GI Model

$D_{s1}(2536)$-D*K
$D_{s2}(2573)$-$D^{(*)}$K
D-wave

Mass stable vs GI model

正宇称的B_s态

Z. Yang, G.-J. Wang, J.-j. Wu, S.-l. Zhu, M. Oka **arXiv:**2207. 07320

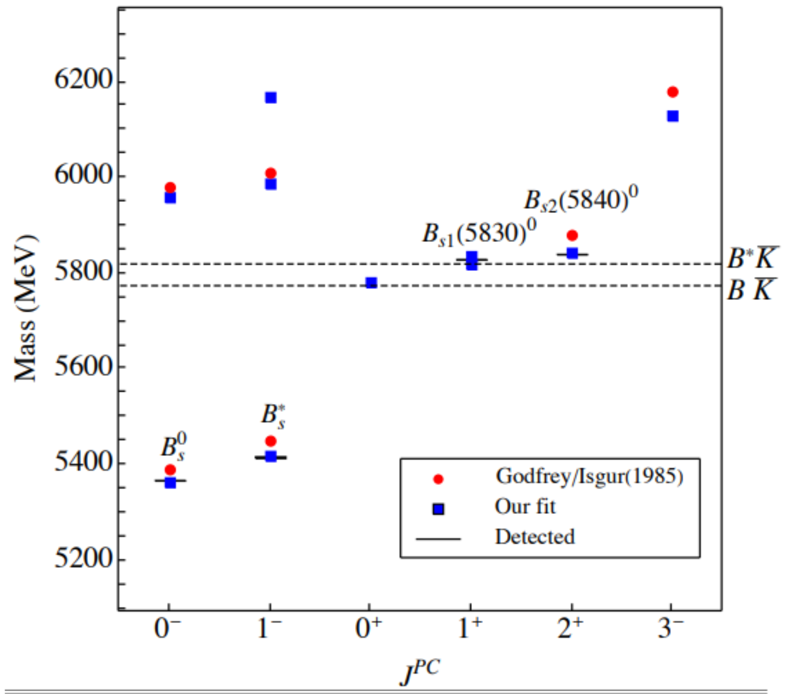

	$b\,(\lvert ^{2S+1}L_J\rangle)$	$b\,(\text{mass})$	α	L
B^*_{s0}	$\lvert ^3P_0\rangle$	5780.9	$B\bar{K}$	S
B^*_{s1}	$-0.74\,\lvert ^1P_1\rangle + 0.67\,\lvert ^3P_1\rangle$ $= 0.98\,\phi_s - 0.22\,\phi_d$	5818.5	$B^*\bar{K}$	$S,\ D$
$B^{*\prime}_{s1}$	$0.67\,\lvert ^1P_1\rangle + 0.74\,\lvert ^3P_1\rangle$ $= 0.22\,\phi_s + 0.98\,\phi_d$	5835.6	$B^*\bar{K}$	$S,\ D$
$B^{*\prime}_{s2}$	$\lvert ^3P_2\rangle$	5842.7	$B\bar{K},\ B^*\bar{K}$	D

$$\frac{1}{4}\left(m_{B_s} + 3m_{B_s^*}\right) = 5403.3\ \text{MeV}.$$

正宇称的B_s态

Z. Yang, G.-J. Wang, J.-j. Wu, S.-l. Zhu, M. Oka **arXiv:**2207. 07320

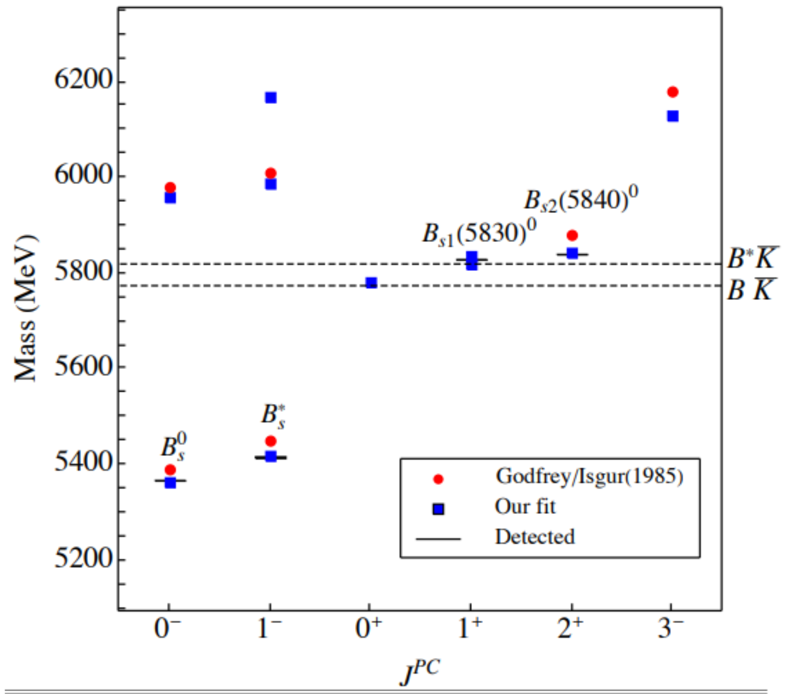

	$b(\vert^{2S+1}L_J\rangle)$	b (mass)	α	L
B^*_{s0}	$\vert^3P_0\rangle$	5780.9	$B\bar{K}$	S
B^*_{s1}	$-0.74\vert^1P_1\rangle + 0.67\vert^3P_1\rangle$ $= 0.98\,\phi_s - 0.22\,\phi_d$	5818.5	$B^*\bar{K}$	S, D
$B^{*\prime}_{s1}$	$0.67\vert^1P_1\rangle + 0.74\vert^3P_1\rangle$ $= 0.22\,\phi_s + 0.98\,\phi_d$	5835.6	$B^*\bar{K}$	S, D
$B^{*\prime}_{s2}$	$\vert^3P_2\rangle$	5842.7	$B\bar{K}$, $B^*\bar{K}$	D

Conclusion:

$B^*_{s0}(5730)-B\bar{K}$

$B^*_{s1}(5770)-B^*\bar{K}$ S-wave

Mass moving vs GI Model

1. Using Previous Parameters

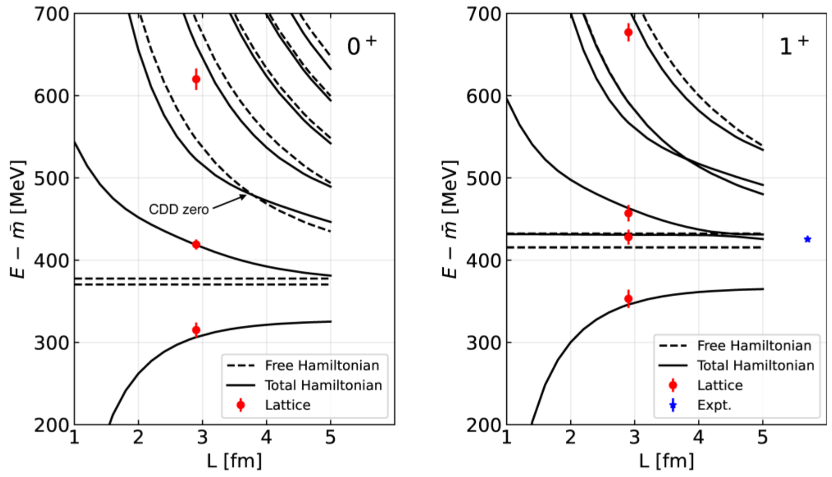

J^P		0^+	1^+
mass [MeV]	rel. quark model [63]	5804	5842
	rel. quark model [64]	5833	5865
	rel. quark model [65]	5830	5858
	nonrel. quark model. [66]	5788	5810
	LO $\chi - SU(3)$ [18]	5643	5690
	Bardeen, Eichten, Hill [89]	5718 ± 35	5765 ± 35
	LO UChPT [24, 25]	5725 ± 39	5778 ± 7
	NLO UHMChPT [30]	$5696 \pm 20 \pm 30$	$5742 \pm 20 \pm 30$
	NLO UHMChPT [90]	5720^{+16}_{-23}	5772^{+15}_{-21}
	HQET + ChPT [67]	5706.6 ± 1.2	5765.6 ± 1.2
	Covariant ChPT [68]	5726 ± 28	5778 ± 26
	local hidden gauge [69]	$5475.4 \sim 5457.5$	$5671.2 \sim 5663.6$
	heavy meson chiral unitary [70]	5709 ± 8	5755 ± 8
	lattice QCD [91]	$5752 \pm 16 \pm 5 \pm 25$	$5806 \pm 15 \pm 5 \pm 25$
	lattice QCD [88]	$5713 \pm 11 \pm 19$	$5750 \pm 17 \pm 19$
	this work	$5730.2^{+2.4}_{-1.5}$	$5769.6^{+2.4}_{-1.6}$
$P(b\bar{s})$[%]	heavy meson chiral unitary [70]	$48.2 \pm 1.5/54.2 \pm 1.1$	$50.3 \pm 1.4/51.7 \pm 1.3$
	this work	$54.7^{+5.2}_{-4.1}$	$56.7^{+4.6}_{-3.7}$

$$\frac{1}{4}\left(m_{B_s} + 3m_{B_s^*}\right) = 5403.3 \text{ MeV}.$$

正宇称的B_s态

Z. Yang, G.-J. Wang, J.-j. Wu, S.-l. Zhu, M. Oka **arXiv:**2207. 07320

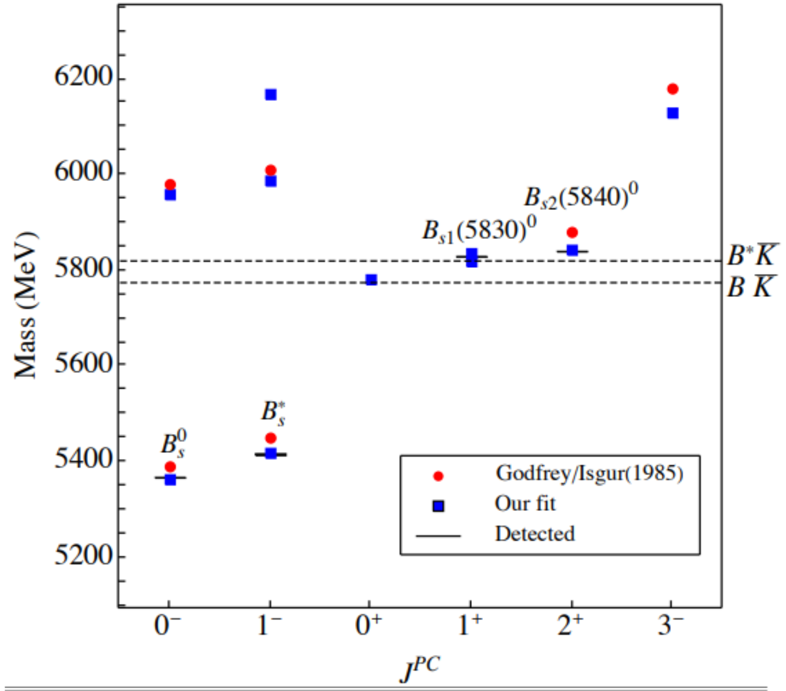

	$b\,(\lvert^{2S+1}L_J\rangle)$	$b\,(\text{mass})$	α	L
B_{s0}^*	$\lvert^3P_0\rangle$	5780.9	$B\bar{K}$	S
B_{s1}^*	$-0.74\,\lvert^1P_1\rangle+0.67\,\lvert^3P_1\rangle$	5818.5	$B^*\bar{K}$	$S,\,D$
	$=0.98\,\phi_s\;-0.22\,\phi_d$			
$B_{s1}^{*\prime}$	$0.67\,\lvert^1P_1\rangle+0.74\,\lvert^3P_1\rangle$	5835.6	$B^*\bar{K}$	$S,\,D$
	$=0.22\,\phi_s\;+0.98\,\phi_d$			
$B_{s2}^{*\prime}$	$\lvert^3P_2\rangle$	5842.7	$B\bar{K},\,B^*\bar{K}$	D

Conclusion:

$B^*_{s0}(5730)$-$B\bar{K}$
$B^*_{s1}(5770)$-$B^*\bar{K}$ S-wave

Mass moving vs GI Model

1. Using Previous Parameters

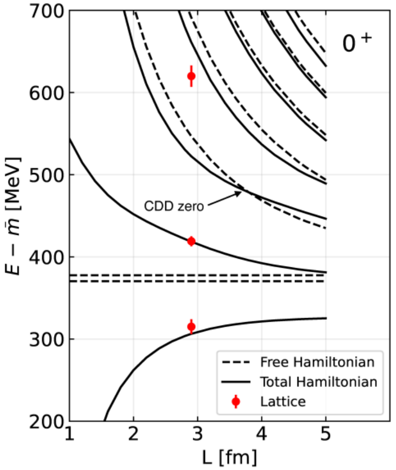

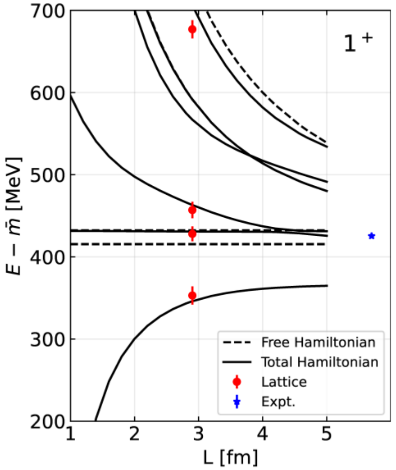

2. A CDD zero

The CDD zero indicates there are two mechanisms which will cancel at this energy.

Give a new method to search CDD zero.

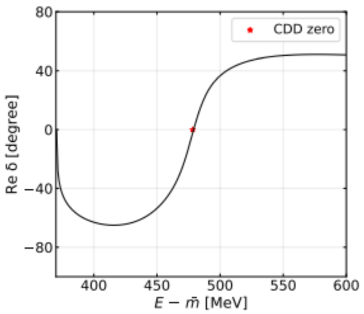

J^P		0^+	1^+
mass [MeV]	rel. quark model [63]	5804	5842
	rel. quark model [64]	5833	5865
	rel. quark model [65]	5830	5858
	nonrel. quark model. [66]	5788	5810
	LO $\chi-SU(3)$ [18]	5643	5690
	Bardeen, Eichten, Hill [89]	5718 ± 35	5765 ± 35
	LO UChPT [24, 25]	5725 ± 39	5778 ± 7
	NLO UHMChPT [30]	$5696\pm20\pm30$	$5742\pm20\pm30$
	NLO UHMChPT [90]	5720^{+16}_{-23}	5772^{+15}_{-21}
	HQET + ChPT [67]	5706.6 ± 1.2	5765.6 ± 1.2
	Covariant ChPT [68]	5726 ± 28	5778 ± 26
	local hidden gauge [69]	$5475.4\sim5457.5$	$5671.2\sim5663.6$
	heavy meson chiral unitary [70]	5709 ± 8	5755 ± 8
	lattice QCD [91]	$5752\pm16\pm5\pm25$	$5806\pm15\pm5\pm25$
	lattice QCD [88]	$5713\pm11\pm19$	$5750\pm17\pm19$
	this work	$5730.2^{+2.4}_{-1.5}$	$5769.6^{+2.4}_{-1.6}$
$P(b\bar{s})[\%]$	heavy meson chiral unitary [70]	$48.2\pm1.5/54.2\pm1.1$	$50.3\pm1.4/51.7\pm1.3$
	this work	$54.7^{+5.2}_{-4.1}$	$56.7^{+4.6}_{-3.7}$

$$\frac{1}{4}\left(m_{B_s}+3m_{B_s^*}\right)=5403.3\ \text{MeV}.$$

Summary

- Introduction of HEFT, until now, it can be applied to calculate the finite volume effect of two body system.
- The study of N*(1535) [3-quark core~50%], N*(1440) [πN–$\pi\Delta$–σN], Λ*(1405) [$\bar{K}N$–$\pi\Sigma$].
- The study of D_{s0}(2317) [$c\bar{s}$-DK(s-wave)], D_{s1}(2460) [$c\bar{s}$-DK*(s-wave)], D_{s1}(2536) [$c\bar{s}$](DK*(d-wave)), D_{s2}(2573) [$c\bar{s}$] DK*(d-wave).
- Predict new B_{s0}(5730) and B_{s1}(5770).
- We can find $q\bar{q}$ and qqq core are always there !
- Interactions between hadrons are always there too !

Outlook

- HEFT combines the Lattice data and Experimental data to constraint the Effective Model, and connects the Quark model (quark level bound state) and Hadron interaction (Hadron level physics), thus provides a complete formalism of physical sates and help us understand the nature of hadron deeply.

Thanks for attention !